EQUAL CHANNEL ANGULAR EXTRUSION OF TUNGSTEN HEAVY ALLOY

A Thesis

by

VENKATA RAVI KIRAN VASIRAJU

Submitted to the Office of Graduate Studies of
Texas A&M University
in partial fulfillment of the requirements for the degree of

MASTER OF SCIENCE

May 2012

Major Subject: Mechanical Engineering

EQUAL CHANNEL ANGULAR EXTRUSION OF TUNGSTEN HEAVY ALLOY

A Thesis

by

VENKATA RAVI KIRAN VASIRAJU

Submitted to the Office of Graduate Studies of
Texas A&M University
in partial fulfillment of the requirements for the degree of

MASTER OF SCIENCE

Approved by:

Chair of Committee,	K. Ted Hartwig
Committee Members,	Ibrahim Karaman
	Peter M. McIntyre
Head of Department,	Jerald Caton

May 2012

Major Subject: Mechanical Engineering

ABSTRACT

Equal Channel Angular Extrusion of Tungsten Heavy Alloy.

(May 2012)

Venkata Ravi Kiran Vasiraju, B.E., Osmania University

Chair of Advisory Committee: Dr. K. Ted Hartwig

Tungsten heavy alloys (WHA's) are composite two phase materials with tungsten particles embedded in an alloy matrix. The alloy matrix can be a binary mixture of Ni with either Fe, Cu, Co or Mn. Owing to their high density and good mechanical properties, these materials are used in a wide range of applications ranging from weights to kinetic energy penetrators. The goal of this thesis was to impart maximum strain to the tungsten heavy alloy via equal channel angular extrusion (ECAE), and evaluate the variation in tungsten particle morphology with level of plastic strain. Severe plastic deformation of tungsten heavy alloys is difficult and challenging.

The WHA used in this project was 90W-8Ni-2Fe. Both high temperature and low temperature ECAE processing were done on this material. Successful multi-pass extrusions were possible only with intermediate annealing at 1300C and at low extrusion rates.

The microstructures of the processed materials were examined using optical and scanning electron microscopy. The recrystallization behavior and hardness variation

with processing were also examined. X-ray diffraction was done to identify the various crystal structures.

Three pass extrusions through a 90 degree die angle ECAE tool (total strain of 3.4) of tungsten heavy alloy were successfully achieved. The previous highest level of total strain imparted to WHA by ECAE was 1.91. The hardness, XRD, and recrystallization results were as expected and in accordance with the results found in the literature. The hardness increases dramatically after the first pass and was nearly the same for the second and the third passes. The tungsten particle morphology obtained after the first and the third pass were as expected. However, the morphology of the tungsten particles after the second extrusion via route C was unusual and "popcorn" like, and of a type not reported previously in the literature. The "popcorn" like morphology of the W phase may give rise to unusual and interesting mechanical properties that should be studied further.

DEDICATION

This thesis is dedicated to the person I love the most, my mother

ACKNOWLEDGEMENTS

I would like to thank Dr. Hartwig for helping me out through the graduate program. He has not only helped through my thesis but also throughout the graduate program as well. He was patient and helped me correct my mistakes. He put a lot of effort and time in my thesis. He played a major part in my thesis and helped me graduate. He has guided me through every step of my thesis and graduate studies. Without his help I would not be submitting my thesis let alone graduating. I am also grateful to my other committee members Dr. Karaman and Dr. McIntyre for their support and guidance in completion of my thesis.

I would like to extend my gratitude to Robert E. Barber, for his help in extrusions and machining; His assistance with machining and extrusions made my thesis possible. I also thank him for all the knowledge he shared with me in many aspects of material science and mechanical engineering. I also thank Doug Krebs for lending his support in different aspects of machining.

I am thankful to David Foley, Shreyas Balachandran, Miao Song and Zach Levin for their help and support in completing my thesis. They helped by giving their valuable suggestions and taught me things necessary for completion of my thesis.

Last but not the least I would also like to thank my parents for their support and encouragement throughout the project. Without their encouragement my success would not have been possible.

TABLE OF CONTENTS

Page

Page

Page

LIST OF FIGURES

Page

Page

Page

LIST OF TABLES

Page

INTRODUCTION

The goal of this project was to impart maximum strain to tungsten heavy alloy via Equal Channel Angular Extrusion and examine the changes in microstructure.

Material

Tungsten heavy alloys typically contain 80 – 98% tungsten alloyed with Ni, Fe and copper [1]. Cobalt, Molybdenum, Chromium etc... are sometimes added as fillers. The density of these materials varies between 16.5 and 18.75 g/cc. They are two phase materials with one phase being tungsten and the alloy being the matrix phase. The alloy phase acts as a binder, holding the brittle particles of tungsten together. Though polycrystalline tungsten is brittle , the alloy matrix gives tungsten heavy alloy, the ductility and toughness [2]. Due to the presence of two phases these materials are sometimes referred to as "genuine composites" [3].

These materials are usually produced form elemental powders, mixed in the required quantities, using powder metallurgy techniques. Liquid phase sintering is by far the most popular technique for consolidation of WHA's [4]. These alloys were initially investigated for their better machinability with lesser emphasis on mechanical properties. But as the need for better mechanical properties increased the emphasis shifted from W-Ni-Cu alloy system to W-Ni-Fe. Delai et al. [5] and Katlin et al. [6] reported that the W-

---

This thesis follows the style of Scripta Materialia.

Ni-Fe system has better mechanical and ballistic properties compared to W-Ni-Cu.

Tungsten Heavy Alloys are extremely sensitive to impurities. Because of this, the early work on tungsten heavy alloys led to disagreement on their mechanical properties. The reported un-worked elongation in "1977 High Density Alloy Conference" varied from 6.6% to 42% [7]. Due to this kind of inconsistency many reported results were considered bad data. But recent developments in powder metallurgy have made production of consistent tungsten heavy alloys possible. These materials are processed between temperatures of 1300^0C – 1500^0C where at least one of the constituents of the alloy melts. Because these materials are manufactured using powder metallurgy techniques, WHA's are for the most part inhomogeneous [4].

WHA materials have a very unique and useful combination of high density, high strength, good ductility, high heat strength, machinability and corrosion resistance. Due to these properties, WHA are used in numerous applications many of which are discussed in the section below.

Applications

Because of the above mentioned special properties of tungsten heavy alloys, these materials are used in a variety of industries ranging from ordnance applications to the medical industry. They are used as kinetic energy penetrators due to their high density, strength and ductility. The other applications of WHA include

- ***Radiation Shielding***: The radiation absorption behavior of WHA is derived from the tungsten phase of the alloy [8]. Because tungsten has high linear absorption

coefficient (better than lead), these materials are used to absorb radiation from modern oncology and radiography systems. They fair better than lead because of their high strength and ductility which gives them a structural advantage compared to lead. Also these materials have lower toxicity making them a more eco-friendly choice [9].

- ***Counter Balance***: These materials are used as counter weights in aircraft and sailboats. They are better than lead because unlike lead, they do not creep under their own weight.

- ***Racing Weights***: Because of their high density and high good structural integrity WHA is also used as ballast in racing vehicles. They are already in use in Nascar weight adjustment tubes. They are used to lower the center of gravity and to increase the stability of the vehicle. Also their high heat resistance makes them more useable at higher temperatures. Due to their high density they occupy less volume for the required weight.

- ***Oil Logging Applications***: Tungsten heavy alloys are excellent materials to be used as casing of down hole logging in oil wells. These materials are heavy enough to sink through oil and mud, materials encountered during drilling, strong enough to with stand high hydrostatic pressure, and hard enough to weather erosion.

- ***Ordnance Applications***: Owing to their excellent mechanical and thermal properties these materials are used for defense application in a number of ways.

They are used to make products ranging from bullets to kinetic energy penetrators to prefabricated fragments and spheres.

Kinetic Energy Penetrators

As the name suggests kinetic energy penetrators are ammunitions which make use of the kinetic energy at the time of impact to penetrate the target. They belong to the category of armor piercing weapons. These are different from bullets used in rifles and pistols. These ammunitions are designed for high energy impact. They travel with a velocity of around 1000m/s. A huge amount of force is generated at the point of impact.

As kinetic energy is a function of mass and velocity of the ammunition, the head of the KE penetrator is generally made of a very dense material. Depleted Uranium (DU) alloys have been used to make these ammunition but due to economic, environmental and safety factors, there is a strong motivation to replace Depleted Uranium with tungsten heavy alloys. But there is still a lack of clarity in the open literature for which material is better compared to other. More on this is discussed in literature review.

Introduction to Severe Plastic Deformation

Severe plastic deformation (SPD) is a process in which a material undergoes intense strain at relatively low temperature [10]. Such processing is considered to be the forefront in the advanced materials. These techniques result in formation of ultrafine grained nano and submicron crystalline structures [11]. Investigations have shown that apart from achieving fine microstructures, materials processed by SPD have unique properties compared to coarse grain structures. Even fundamental properties like elastic

moduli, saturation magnetization, curie and debye temperature have been reported to change after severe plastic deformation [11]. It is considered to be the best technique to achieve nano and submicron grained structures from the top-down approach.

There are many techniques which can be used to get nano structures but SPD is better because it eliminates some of the problems posed by the other techniques which use the bottom-up approach. For example porosity can be eliminated which is a major problem in powder compaction. Also pure samples which are larger in size and practical can be processed using SPD.

There are different SPD techniques. High Pressure Torsion (HPT), Equal Channel Angular Extrusions (ECAE), Multi-directional forging, Cyclic Extrusion Compression, Twist Extrusion, and Accumulative Roll Bending are some of the SPD techniques.

High Pressure Torsion

High Pressure Torsion is a process in which torsion is applied to a thin disk under high pressure. This process applies large strains on the material without fracturing it, as in ordinary torsion tests due to the application of high pressure. The effect of torsion and high pressure leads to intensive angular deformation [12].

High strains can be imparted to a material using high pressure torsion. Ultrafine grain materials of high quality can be fabricated using this technique. But the main drawback of this SPD processing technique is the limitation it imposes on the sample size. Very think disks (~10μm) can only be processed by this technique.

Twist Extrusion

It was first proposed by professor Beygelzimer, and is a relatively new SPD technique [13]. In this process the billet is extrudes through a die which has a twisted channel. The channel has the same cross section throughout its axis. The schematic of this technique is shown in Figure 1. Though this material imparts high strain to materials, the need for complicated tooling limits its usage.

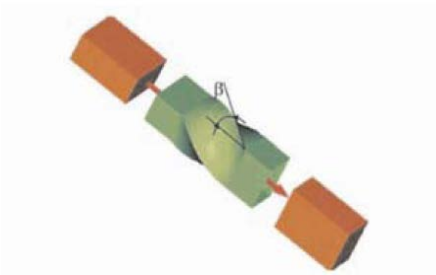

Figure 1 Schematic of twist extrusion [13]

Accumulative Roll Bending (ARB)

In this process two sheets of the same thickness are joined in thickness and rolled together. In one pass they are rolled to the thickness of original sheet. Then the sheet is again divided into two pieces and these are rolled together. The need to cut the material before every pass is a problem. Also the need to advanced tooling limits its possibility[14].

Of all the SPD techniques ECAE is the most popular SPD [15] technique. This process is described in the next section and also its advantages over other SPD processing techniques.

Equal Channel Angular Extrusion (ECAE)

ECAE was first reported by Segal in 1972 [16].It was reported that simple shear was the ideal deformation method. Equal Channel Angular Extrusion (ECAE) uses the principle of simple shear which was reported to be ideal deformation method for microstructure refinement and texture development. The equal channel angular extrusion tool consists of two channels with identical cross section, with their axis aligned at an angle to each other. A lubricated work piece or the "billet" is pushed through these channels. Simple shear deformation is achieved in a thin region at the plane of crossing of the channels as shown in Figure 2. The applications of this process are listed in the next section.

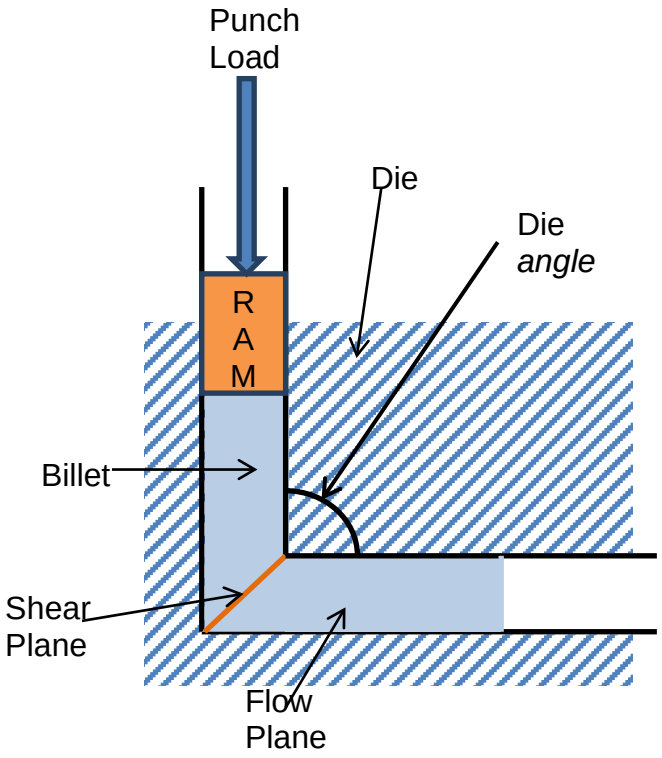

Figure 2 Schematics of equal channel angular extrusion

Applications of ECAE

There are numerous applications for ECAE, including material synthesis and processing. A number of metals can be processed using this technique. ECAE has been found to be useful in to improve and refine the microstructure of many metals. ECAE can also be used to introduce texture in metals to get required anisotropic properties. Successfully processed materials include copper [17], aluminum, nickel, iron, magnesium, tantalum, tungsten, titanium and many more alloy systems.

ECAE can also be used to consolidate amorphous metal powders to produce bulk metallic glasses. A large number of metallic powders can be processed using this process. Production of sub-micrometer or micrometer grain size in high purity Al, Cu and Ti for sputtering targets, is one of the applications. Other applications include production of ultrafine-grain structures in bulk materials.

Grain Refinement

Among the various techniques available for refining the microstructure of a material ECAE holds the edge for the following reasons

- A variety of materials can be processed
- Large rods, bars, plates and sheets can be extruded
- Reasonable homogeneity is attained
- Scale up for large samples is possible
- Can be used for all materials ranging from metals to metal - metal matrix composites

Texture Development

As mentioned above in previous sections ECAE imparts intense strain to a billet without any appreciable change in its cross section area. Because of this it is easier to impart moderately to strong texture on the billets. Also the availability of different routes to work with in ECAE allows for attainment of different textures in a material [18]. As texture development plays a role in grain refining process [19], the possibility of multiple passes makes it more advantageous.

Powder Compaction

ECAE can also be used for powder compaction of amorphous metals. Due to the possibility of multiple routes, better compaction is achieved in ECAE compared to other SPD techniques. The successfully processed powder via ECAE include aluminum, copper, copper blended with silver, tin copper and aluminum blend, amorphous copper and zirconium alloy, and many more.

THESIS OVERVIEW

Tungsten heavy alloy (WHA) is a difficult to process material; strain rate sensitive with a significant amount of shear localizing capability and shows ductility exhaustion after strains of 20 – 30%. The goal of this project is to process tungsten heavy alloy, by severe plastic deformation such that maximum strain is imparted to it without fracture. In this project a strain greater than 3 is the target.

The aim of the processing is to refine the grain structure, change the morphology of the tungsten particles and increase the hardness of the material. The deformation method to be used is equal channel angular extrusion (ECAE). To determine the thermo-mechanical processing parameters the recrystallization behavior and the phase changes with respect to heat treatment are studied.

LITERATURE REVIEW

Tungsten Heavy Alloys

The material used in this research belongs to tungsten-iron-nickel group. For this project the material had nominal composition of 90% tungsten, 8% Ni and 2% Iron. The W-Ni-Fe group of alloys are considered to have better mechanical properties than W-Ni-Cu alloys [20], and so were used in this study. These heavy density metals were be manufactured by liquid phase sintering [21]. These materials have a density of about 17 g/cc.

These are two phase materials with tungsten forming one phase and Ni-Fe alloy forming the other. The Ni-Fe acts as a binder holding the tungsten phase together. A typical microstructure of tungsten heavy alloy is shown in Figure 3. The different alloy systems which belong under the category of tungsten heavy alloy are discussed next.

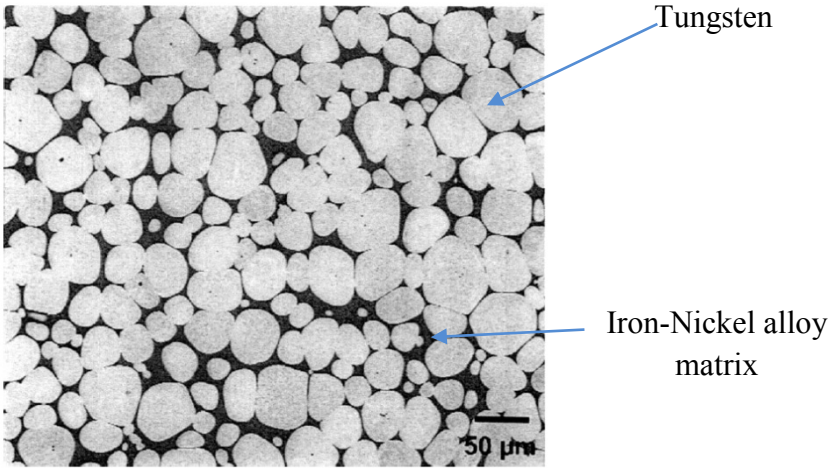

Figure 3 SEM picture of a typical microstructure of Tungsten Heavy Alloy [4]

Other Alloy Systems

The different alloys which constitute tungsten heavy alloys are

- Tungsten – Nickel – Iron (W-Ni-Fe)
- Tungsten – Nickel – Copper (W-Ni-Cu)
- Tungsten – Nickel – Manganese (W-Ni-Mn)
- Tungsten – Nickel – Cobalt (W-Ni-Co)
- Tungsten – Hafnium (W-Hf)
- Tungsten – Titanium (W-Ti)

Tungsten – Nickel – Copper

These alloys are sintered at higher temperatures than tungsten – nickel – iron alloys [22]. These alloys have inferior mechanical properties compared to Ni-Fe alloys. The tungsten – nickel – copper alloys tend to have more pores than tungsten – nickel – iron alloys which contribute to their poor performance in mechanical properties. Also because the tungsten – nickel – copper alloys are sintered at higher temperatures compared to tungsten – nickel – iron alloys. Tungsten – nickel – copper alloys have coarser tungsten grain which again leads to its poor mechanical properties. Under uni-axial tension the tungsten – nickel – copper alloys fail by matrix-interface fracture whereas the tungsten – nickel – iron alloys fail by W-grain cleavage.

The comparison of Tensile strength and % Elongation, between W-Ni-Cu and W-Ni- Fe alloys is shown in Figure 4 and Figure 5.

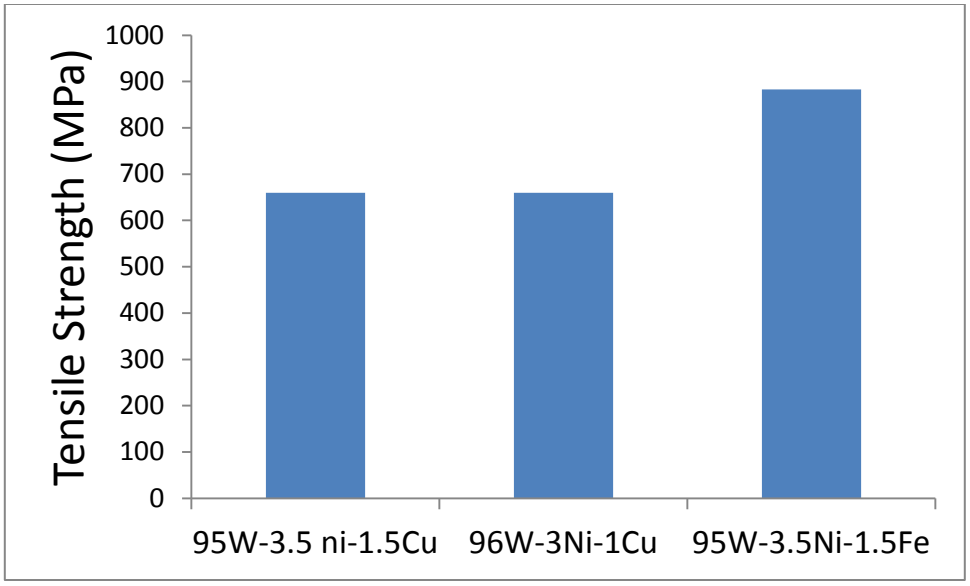

Figure 4Comparison of tensile strength between W-Ni-Cu and W-Ni-Fe alloys [22]

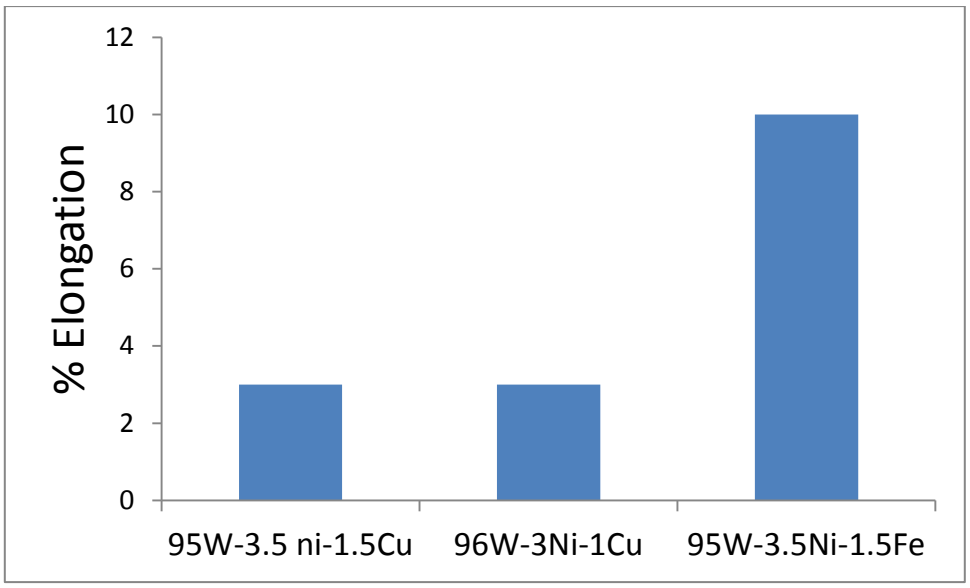

Figure 5Comparison of % elongation between W-Ni-Cu and W-Ni-Fe alloys [22]

Tungsten – Nickel – Manganese

The tungsten nickel and manganese alloys have a lower sintering temperature than most of the tungsten heavy alloys [23]. The sintering temperature of these alloys is 300^0C less than that of W-Ni-Fe alloys. The down side to these alloys is the porosity in the material and oxidation of manganese at sintering temperatures. Also during sintering manganese evaporation is a problem to achieve high densities. German [24] concluded that the mechanical properties of these materials are close but inferior to the W-Ni-Fe alloys.

Tungsten – Nickel – Cobalt

Tungsten – Nickel – Cobalt alloy belongs to the class of tungsten heavy alloy. Their mechanical properties were reported by Couque et al. [25], Lankford et al. [26] and Muresan [27]. It was concluded that the cobalt alloy was superior in tensile strength but inferior in ductility. This behavior is shown in Figure 6. The down side to tungsten alloy is that cobalt is a carcinogenic material. It decreases the solubility of tungsten in the matrix phase.

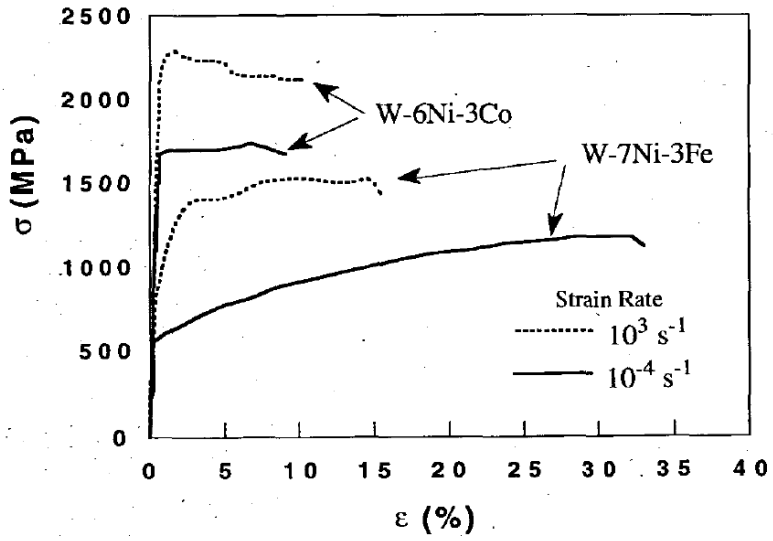

Figure 6 Comparison of stress-strain curves of W-Ni-Co and W-Ni-Fe alloys [27]

Many other alloys are also considered as tungsten heavy alloys, but these are not discussed here because they are not of much practical significance [28, 29].

Processing

Tungsten belongs to the class of refractory metals, and has a melting point of about 3400C. Conventional methods of manufacturing tungsten heavy alloys are not practical, owing to their high melting point. Powder metallurgy techniques are used to manufacture the alloys. Among different powder metallurgy techniques liquid phase sintering is the most popular one.

Liquid phase sintering provides near theoretical densities, homogenous microstructures and enhanced densities at lower processing temperatures [30].

The tungsten in tungsten heavy alloys is soluble in the alloy melt. This causes the preferential dissolution of sharp edges and gives rise to the smooth and rounded corners as shown in Figure 3. The tungsten which dissolves in the alloy re-precipitates on a different tungsten particle. This mechanism is called solution-reprecipitation or Ostwald ripening [31]. The typical stages during liquid phase sintering are as follows

- Rearrangement
- Solution-reprecipitation
- Grain-shape
- Accommodation
- Ostwald ripening
- Coalescence

These stages often overlap. This leads to the modification of microstructure and densification of the alloy. Typical grain size of tungsten varies from 20 – 60 μm.

Due to the huge differences in densities of tungsten and the alloy phases the liquid phase should be less than 20%. If the difference is more than 20% it leads to inhomogeneous microstructures, non-isotropic properties and segregation as shown in Figure 7, which shows an inhomogeneous microstructure of 78W–15.4Ni–6.6Fe WHA alloy segregated due to gravity.

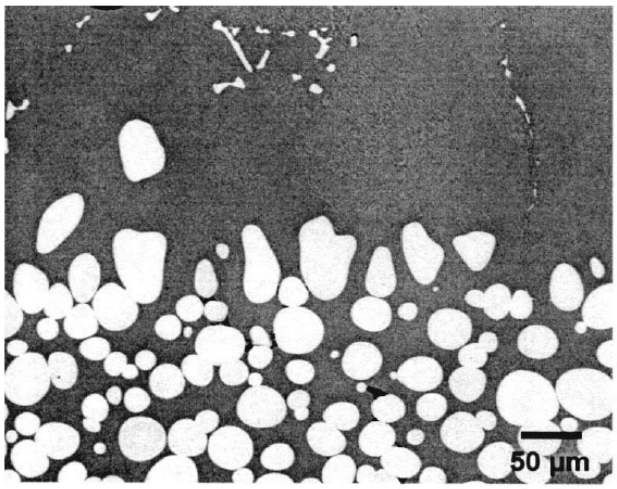

Figure 7 Inhomogeneous microstructure of 78W–15.4Ni–6.6Fe [4]

Also these materials are post sintered to eliminate some of the problems which creep in due to Liquid phase sintering, mentioned above.

Material Properties

The mechanical properties of tungsten heavy alloys are dependent on many factors. The mechanical properties are extremely sensitive to impurities. Even the alloys of same composition made with the same PM technique with the same variable, but made by different research groups have different properties [1]. This was evident during the "High density metals conference" held in 1977 where the reported ductility of the same alloy system as reported varied from 6%-40% [7].

The mechanical properties of these alloys also depend on the following factors [32].

- Composition of the individual elements in the alloys
- Sintering temperatures and times

- Sintering atmospheres
- Cooling rates
- Residual porosity
- Hydrogen embrittlement
- Impurity segregation
- Pre-processing
- Manual skill and dexterity

Because all these factors influence the mechanical properties, it is difficult to present any literature review on the mechanical properties of these materials. This problem is also compounded by the fact that most the studies are done on alloy systems which have Ni-Fe in the ratio of 7:3. The alloy system used in this study has Ni-Fe ratio of 8:2. There is a dearth of literature on mechanical properties or ballistic properties of 90W-8Ni-2Fe. The only work which was published on this alloy system was by Spencer et al [1]. They suggested that the present alloy system be used in this thesis i.e. 90W-8Ni-2Fe, is better suited for kinetic energy penetrators, but because of a lack of time these properties were not studied in this report. It is a little strange that many researchers pursued the alloy systems with Ni-Fe ratio of 7:3 when the above work clearly mentioned that the 8:2 systems are better. This work was published as early as 1991.

Recrystallization Behavior

As mentioned in the previous section, there is a dearth of literature on 90W-8Ni-2Fe alloy. There is no published information about the recrystallization behavior of this

alloy. A review on recrystallization behavior of other tungsten alloys was done. We estimated that behavior of material used in this thesis is somewhat similar to what is found in the literature for other tungsten heavy alloy of the same class (W-Ni-Fe). The specifics may be a bit different but the trend should be similar.

Ekbom et al. [33], reported on the recrystallization behavior of 90W-7Ni-3Fe alloy. To deform the alloy, 24%, 49% and 57% area reduction was achieved through isostatic extrusion at 400C. Heat treatments were preformed from 700C-1100C. The micro-hardness of these materials at various temperatures is shown in Table 1.

Table 1 Micro-hardness (H_V) of tungsten particles in heat treated tungsten heavy alloy (90W-7Ni-3Fe) [33]

Temperature (°C)	Area reduction			
	0%	24%	49%	57%
25	389 ± 13	440 ± 13	506 ± 12	509 ± 11
700		443 ± 20	512 ± 13	509 ± 20
800		482 ± 23	540 ± 28	526 ± 13
900		429 ± 18	497 ± 19	495 ± 17
1000		394 ± 15	489 ± 16	471 ± 23
1100		390 ± 10	419 ± 14	441 ± 15

The recrystallization curve for the same alloy is shown in Figure 8.

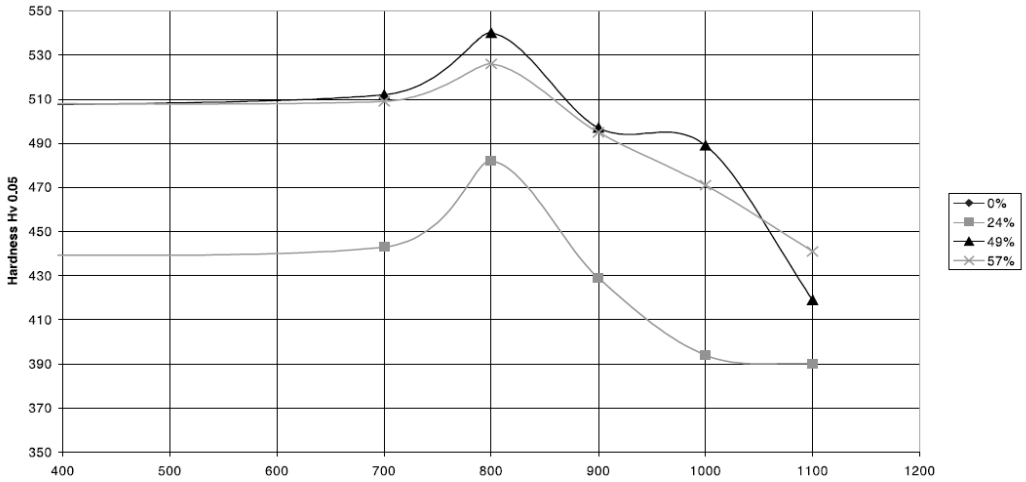

Figure 8 Recrystallization curve for 90W-7Fe-3Ni alloy [33]

From Table 1and Figure 8we can see that the hardness of the material is relatively unchanged with a value of 510HV for 49% and 57% deformation and 440 HV for 24% area reduction, till 700C. The hardness reached a peak at 800C at 540, 529 and 480HV for 57%, 49% and 27 % area reduction. As the temperature increased further, the harness decreased and at 100C the hardness of the recrystallized samples reached close to that of the un-deformed samples of 390 HV.

Mechanical Properties

In this section some properties presented by Spencer at al. are reviewed. This group looked into a variety of aspects which change the mechanical and ballistic behavior of tungsten heavy alloys ranging from effects of impurities to the effect if alloy composition and other variables. In this section the mechanical properties of tungsten heavy alloys for different elemental compositions are reviewed and compared against the material used for this project (90W-8Ni-2Fe).

Un-worked Mechanical Properties

The different mechanical properties i.e. tensile strength, yield strength, elongation, impact energy and hardness of un-worked materials are presented in Table 2.

Table 2 Mechanical properties of different un-worked tungsten heavy alloy systems [1]

Alloy System	Ni:Fe	Avg UTS (Ksi)	Avg YS (Ksi)	Avg Elongation	Avg Hardness (HRC)	Avg impact energy (Ft-lbs)
90W-7Ni-3Fe	7:3	136	85	34	31.0	32
90W-8Ni-2Fe	8:2	140	86	38	30.0	47
93W-4.9Ni-2.1Fe	7:3	140	88	32	31.8	19
93W-5.6Ni-1.4Fe	8:2	140	87	34	31.2	31
96W-2.8Ni-1.2Fe	7:3	140	88	23	31.6	8.1
96W-3.2Ni-0.8Fe	8:2	141	87	25	31.6	12

The UTS, yield strength, and hardness of these materials changes ever so slightly as the % tungsten changes. But the impact energy on 90W-8Ni-2Fe system is superior compared to other systems. The authors claim that many impact specimens of these materials pulled through the fixture without breaking into two. This demonstrates that the ductility of this system is superior to other systems.

Worked Properties

Mechanical properties of different allot systems were evaluated after swaging to at 8, 15 and 25% area reduction. The results are shown in Table 3. Defects like voids in the microstructure and micro cracks, were observed of these materials were swaged above 25%. But in alloys with 8:2 ratio of Ni:Fe defects were not observed. It can be seen from Table 3 that the hardness drops a little after 8% swaging but the % elongation decreases. The impact energy is not dramatically affected, though this decreases slightly.

Table 3 Mechanical properties of worked tungsten heavy alloy systems [1]

Alloy System	Ni:Fe	% Swaging	Avg UTS (Ksi)	Avg YS (Ksi)	Avg Elongation %	Hardness HRC	Impact Energy (ft-lbs)
90W-7Ni-3Fe	7:3	8	156	143	21	41.3	15
		15	166	153	17	42.5	18
		25	181	171	11	42.7	10
90W-8Ni-2Fe	8:2	8	159	148	20	40.1	22
		15	168	156	20	40.5	26
		25	177	165	16	41.7	26
93W-4.9Ni-2.1Fe	7:3	8	161	147	17	41.9	8.6
		15	169	156	12	42.5	9
		25	183	170	11	43.5	9.5
93W-5.6Ni-1.4Fe	8:2	8	164	150	20	38.9	17
		15	171	156	14	40.3	17
		25	181	172	14	42.7	17

Table 3 continued

Alloy System	Ni:Fe	% Swaging	Avg UTS (Ksi)	Avg YS (Ksi)	Avg Elongation %	Hardness HRC	Impact Energy (ft-lbs)
96W-2.8Ni-1.2Fe	7:3	8	165	153	9	42.8	2.7
		15	174	161	8	44.5	2.6
		25	186	178	5	45	0.9
96W-3.2Ni-0.8Fe	8:2	8	161	150	13	40.6	6.6
		15	172	158	9	41.5	4.1
		25	178	164	7	42.7	3.3

The various ballistic tests done by the authors on this project showed that, for 20mm and 30mm phalanx ballistic testing, the alloys with 8:2 ratio of Ni:Fe were superior compared to 7:3. From the mechanical and ballistic testing, 8:2 ratio alloys were concluded to have superior properties than 7:3. Also 8:2 materials had fewer defects and have better workability. So 90W-8Ni-2Fe was used for this project.

Kinetic Energy Penetrator

Kinetic energy penetrators are ammunition which use kinetic energy to defeat a armor and destroy the target. The key requirements for kinetic energy penetrators are good penetration and high density of the material used. The high density enables delivering higher kinetic energy. Penetration is evaluated as the diameter of the tunnel formed in the armor plate during the impact of penetrator with an armor [34]. It was evaluated that the material used for a kinetic energy penetrator should have a ductility ranging between 6 – 8 % and a toughness of 33MPa [35]. The impact velocities of these materials lie between 1000 – 2000 m/sec.

The conditions experienced by a kinetic energy penetrator at the time of impact are very severe. They experience a temperature rise to 2000C approximately, a shear strain in the range 106range and a hydrostatic pressure of 2 – 6Gpa [36]. Because of the high temperatures and strain rates involved there are two competing mechanisms which take place during the impact. These mechanisms influence the performance of the penetrator. Due to the high temperature and high strain rate, the rate of heat transfer is so low that the deformation here can be regarded as adiabatic. Thermal softening occurs due to high rise in temperature and also there is hardening arising from high strain rates and severe plastic deformation. At the point of impact the thermal softening competes with the strain rate hardening. The shear deformation here should be such that adiabatic shear bands form leading to a “self-sharpening” behavior as opposed to gross plastic deformation and mushrooming. The self-sharpening behavior leads to better penetration performance. The ideal properties of a KE penetrator are shown in Table 4.

Table 4 Requirements for a kinetic energy penetrator [4]

Attribute	Function
High density	Imparts high impact energy
No intermetallic phase	Avoids poor interfacial bonding
High strength	For greater heat generation for a given strain
Low heat capacity	Heat generated results in rapid temperature rise
Low work-hardening rates	Easier flow softening
Low strain-rate hardening rates	Shear localization occurs at lower strains
High thermal-softening rate	Shear banding initiated at lower temperature

Conventionally depleted uranium alloys have been the material of choice for kinetic energy penetrators, because of their high density and self-sharpening behavior. But when these materials were used in the gulf war in 1991, there was an immediate response from the general public, anti-nuclear activists and environmentalists [37]. The reaction was against the use of depleted uranium, a radioactive material, as a weapon of war, this lead to medical, environmental, humanitarian, legal technical and political oppositions. Many materials were then looked at for their use as a kinetic energy penetrator. A comparison of limit velocities (i.e. the minimum velocity required for a KEP to penetrate the standard rolled steel armor) and densities of various materials is made in Figure 9. Among all the choices tungsten heavy alloys emerge as a viable choice for material for kinetic energy penetrators.

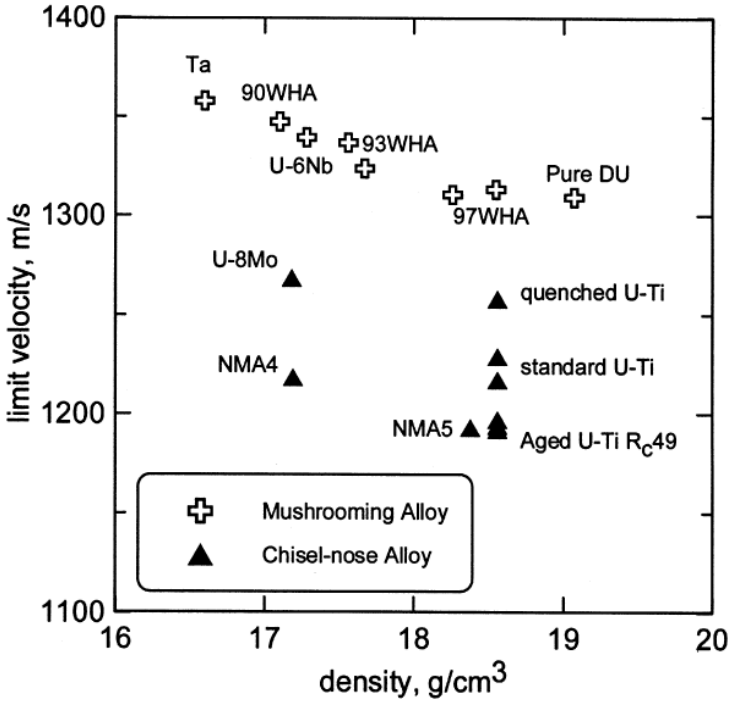

Figure 9 Comparison of density and limit velocities of various materials [38]

Tungsten Heavy Alloy as Kinetic Energy Penetrator

As mentioned in previous sections the KE penetrator experiences severe conditions during the time of impact. Self-sharpening behavior is required for better penetration performance of KE penetrators. DU alloys are known for their self-sharpening or chiseling effect, whereas tungsten heavy alloys are known for their mushrooming. Due to the high melting point the thermal softening effect of WHA is low; this delays the onset of shear localization causing the tungsten alloy heads to deform i.e. mushrooming. This causes considerable dissipation in KE and therefore lower penetration. The head deformation of both these materials is shown in Figure 10. In Figure 11, a comparison of penetration is made for DU and tungsten heavy alloy.

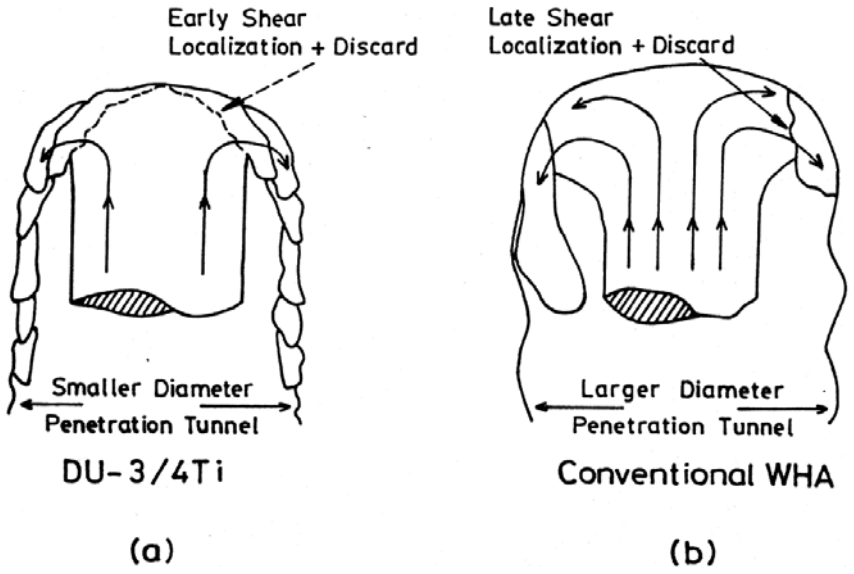

Figure 10 Penetrator deformation showing the penetration behaviour of a) depleted uranium alloy and b) tungsten heavy alloy [39]

Though tungsten heavy alloys do not match up as KE penetrators compared to DU alloys, recent developments and the current research for use of tungsten heavy alloys, indicate that WHA can be as good as DU alloys [37]. The fact that tungsten heavy alloys are not radioactive makes them cheaper to manufacture because the handling is trouble free compared to DU alloys [28].

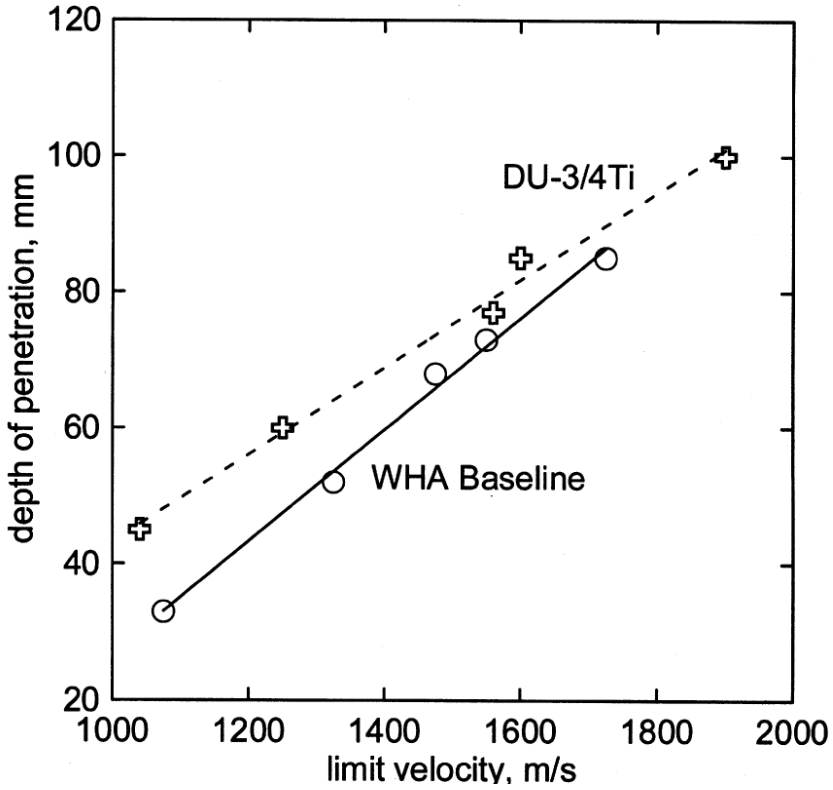

Figure 11 Penetration properties of DU and tungsten heavy alloy [39]

Processing of WHA

Tungsten and tungsten heavy alloys are one of the most difficult metals to process. As the amount of tungsten in tungsten heavy alloy increases, the machinability and the ability to plastically deform decrease [40]. There is a good amount of literature found on sever plastic deformation of tungsten and tungsten heavy alloys.

Wei et al published reports on ECAE and HPT processing of tungsten metal [41-44]. Valiev et al. worked not only on ECAE of tungsten but also on ECAE of tungsten heavy alloy [45]. This is the only published work on ECAE of tungsten heavy alloy that was found.

In this project ECAE was used as the severe plastic deformation technique for microstructure refinement and homogenization of WHA materials. The next section reviews some fundamentals of ECAE.

ECAE Literature Review

Equal channel angular extrusion (ECAE) is one of the severe plastic deformation techniques. It was first discussed in the open literature in 1972. ECAE uses the concept of simple shear deformation, which is "near ideal" deformation method for microstructure and texture development. The equal channel angular extrusion tool consists of two channels with identical cross section, with their axis aligned at an angle to each other. A lubricated work piece or the billet is pushed through these channels. Simple shear deformation occurs at the plane of crossing of the channels. Figure 12 shows the concept of ECAE. The strain intensity ($\Delta\varepsilon_i$) undergone by the material in a single pass is given by

$$\Delta\varepsilon_i = \frac{2}{\sqrt{3}}\cot\varphi \quad \text{.....1}$$

where 2φ is the angle between the axis of the channels. The strain intensity ε_n for N number of passes is given by

$$\varepsilon_n = N\frac{2}{\sqrt{3}}\cot\varphi \quad \text{.....2}$$

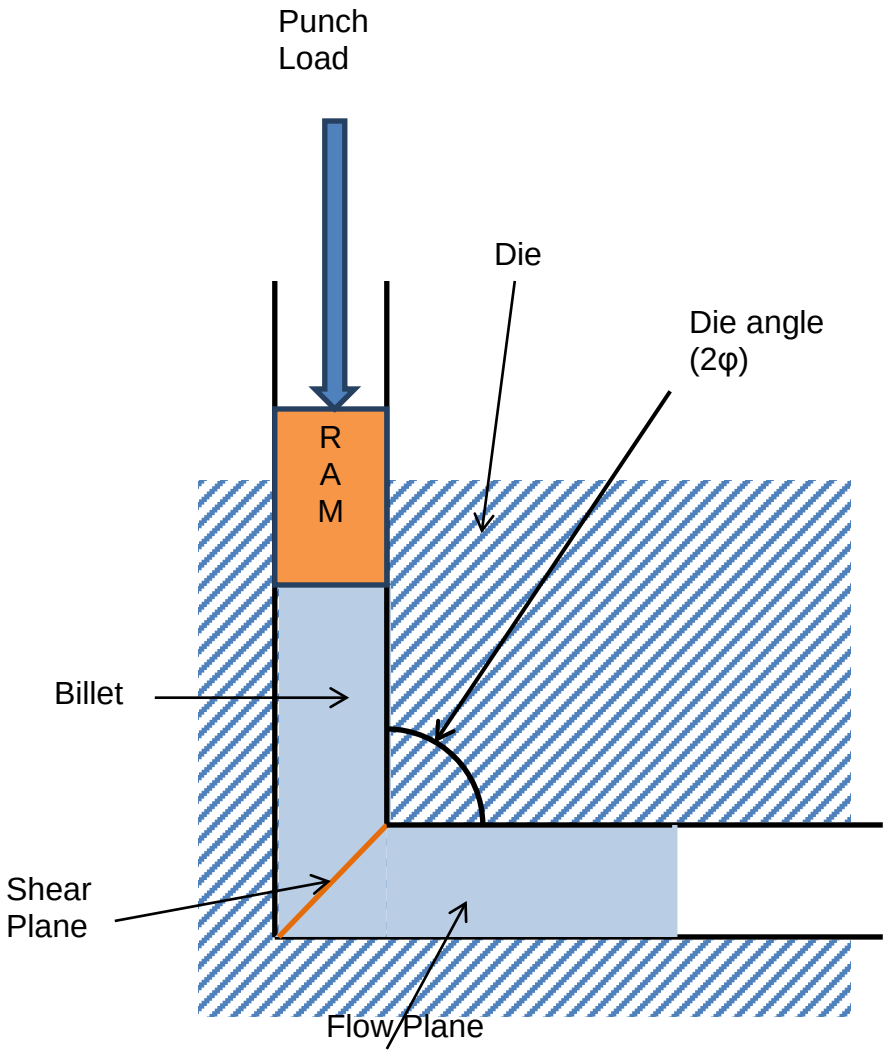

Figure 12 A schematic of ECAE

After extrusion, the whole billet is uniformly deformed with the exception of small end zones. Also during extrusion, the billet does not necessarily follow the sharp corners of the die but tend to round off. This gives rise to fan angle and simple shear deformation occurs to a degree, over this angle. This is not considered in the formulation of strain intensity presented here.

From equation 2 it is obvious that the strain intensity increases as the number of extrusions/passes increase. The strain intensity and equivalent reduction in area, for different number of passes, for a 90^0 die is shown in Table 5.

Table 5 Strain intensity and equivalent reduction in area as a function of number of passes for 90 degree die

Number of passes	Total strain intensity	Equivalent Reduction in Area
1	1.15	69
2	2.31	90
3	3.46	97
4	4.62	99
5	5.77	99.7
6	6.93	99.9
7	8.09	99.97
8	9.24	99.99

From Table 5 it is evident that to get the strain intensity achieved in 8 passes without any change in the cross-section dimensions through ECAE is equivalent to reducing the area

by 99.99%. This is one of the major advantages of ECAE. The multi pass capability without change in the cross-section sets ECAE apart from other deformation techniques. This gives rise to some unique capabilities in achieving texture and micro structure. The billets can be processed in several routes. There are four fundamental routes through which the material can be processed. They are named Route A, Route B, Route C and Route B_C.

Route A: In this route the orientation of the billet is conserved between the passes.

Route B: The billet is rotated $+90^0$ and -90^0 alternatively along the longitudinal axis after each pass.

Route C: In this the billet is rotated 180^0 after each pass.

Route D or B_C: After each pass the billet is rotated 90^0.

The schematic of different routes is shown in Figure 13.

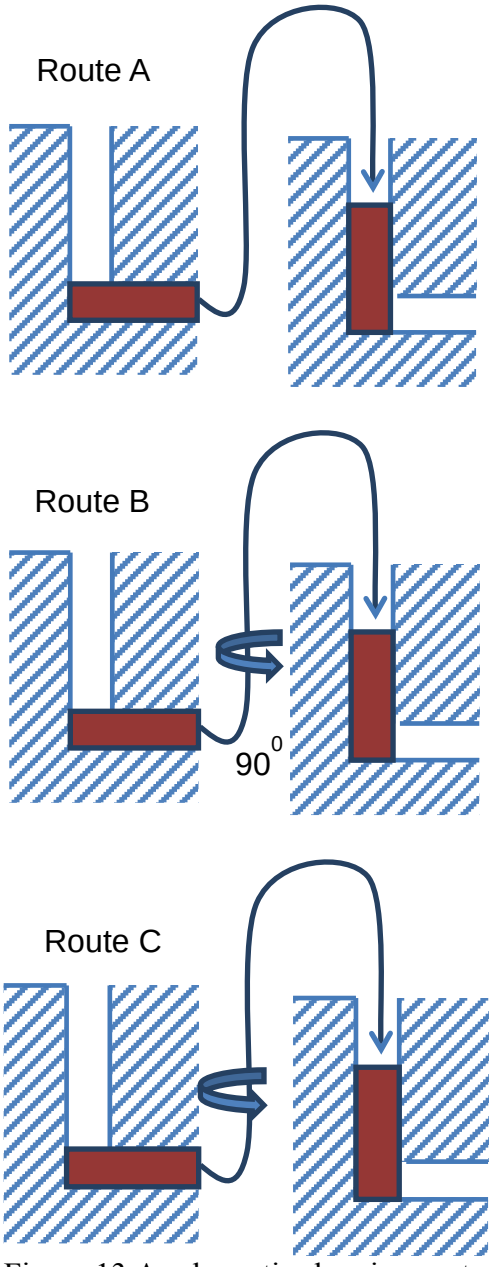

Figure 13 A schematic showing routes A, B and C during ECAE

The element distortion in different routes is shown in Figure14. Material elements are distorted in routes A and B, for plane and spatial flows. In routes C the elements are

restored after 2 passes and in route D or B_C the elements are restored after 4 passes. Also for route A and C, the plastic flow is plane. Each route gives different texture, microstructure and properties. So it is important to design the process so as to optimize the number of passes.

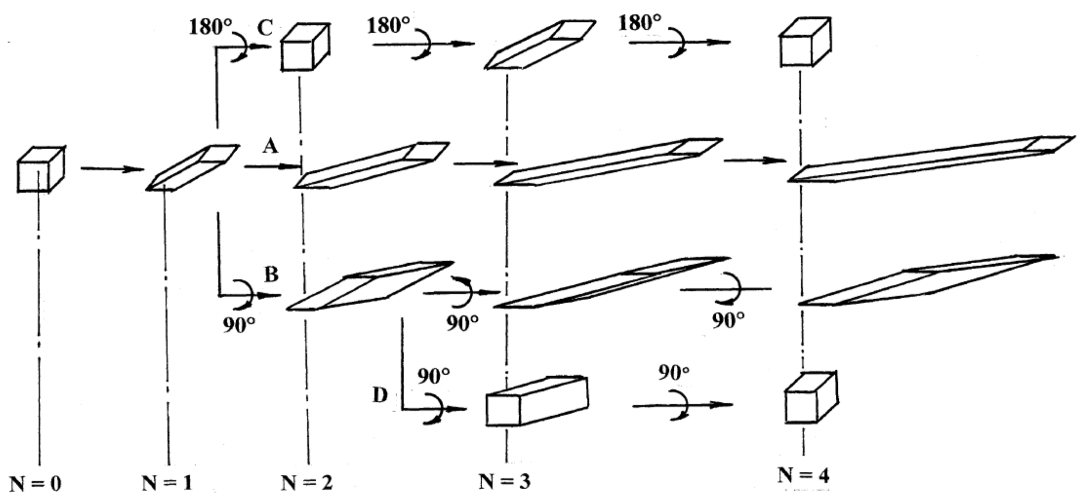

Figure 14 Material element distortion in routes A, B,C and Bc [46]

Route A

As mentioned for this route the orientation of the billet stays the same for all the passes. The elemental distortion keeps increasing as the number of passes increase. This is shown in Figure 15. The total elemental shear (γ) is given by

$\gamma = \tan \Psi = 2N \cot \varphi$ ....(3)

Here Ψ is the angle the element makes with the perpendicular to the billet axis as shown inFigure15. N is the number of passes and 2φ is the angle made by the intersecting channels.

The aspect ratio of the elements deformed (M), the ratio (S) of deformed elements surface area (SN) to the initial element surface area (SO) and the angle of element inclination (θ) to billet axis are given in terms of total elemental shear as below.

$$M = \gamma^2 + 1$$

$$\tan\theta = (\gamma + 1)^{-1}$$

$$S = \frac{1}{3}[2+(\gamma^2+1)^{1/2}]$$

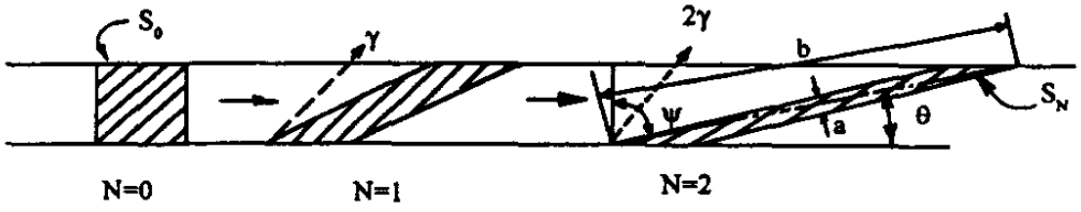

Figure 15 Material element distortion for route A [47]

ECAE of WHA

Vailev et al. published a report ECAE of tungsten heavy alloys [45]. Tungsten heavy alloy with a composition of W-4.3Ni- 2Fe was used. This material posed a many processing problems. When a 120^0 die was used the billet failed after one or two passes. To successfully process these materials through ECAE, a special die with a 135^0 die angle with back pressure was used. Using this die four passes were achieved at 1100C on this material. The die used is shown in Figure 16.

Figure 16 135 degree die used for processing WHA by Valiev [45]

The material was processed in route C. The microstructures before and after processing are show in Figure 17.

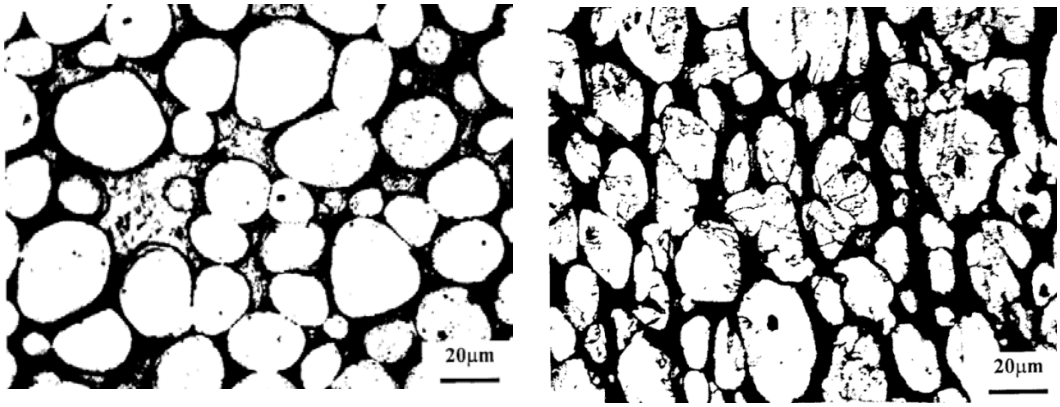

Figure 17 Microstructure of a) as received and b) 4C processed WHA [45]

Other Works on Tungsten Heavy Alloy

In this section a review of literature on mechanical and thermo-mechanical processing of WHA alloy relevant to this project is reviewed. Baek at al. [48] worked on the heat treatment behavior of 93W-4.9Ni-2.1Fe tungsten heavy alloy. The goal of their project was to increase the impact energy of tungsten heavy alloy. The alloy was cyclically heat treated to a temperature of 1150C. This changed the shape of the tungsten grains in the

alloy. The impact energy increase was three fold, from 57 to 170 J. It was concluded that the shape change of tungsten grains “undulated” grains was because of the difference in thermal expansion coefficient of the tungsten and matrix phase. The microstructures of as-received and heat treated tungsten heavy alloy is shown are shown in Figure 18. The alloy was cyclically heat treated 20 times with sintering a 1485C when needed.

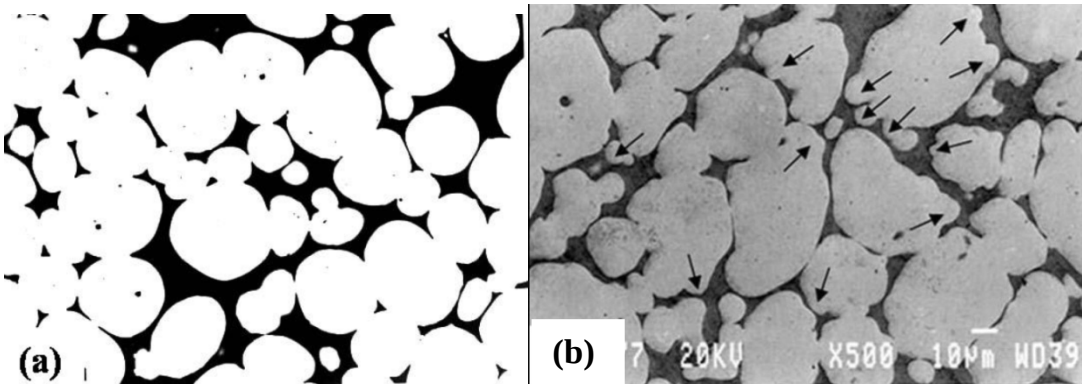

Figure 18 Microstrucutres of a) as received and b) cyclically heat treated tungsten heavy alloy [48]

Strain Rate Deformation

The strain rate deformation of 90W-7Ni-3Fe tungsten heavy alloy was reported by Coates et al. [49]and German et al. [50]. Coates reported that, during kolsky bar tests, adiabatic shear localization developed for a strain rate above 260/s. But at lower strain rates, it was possible to impart shear deformation. Figure 19 shows the adiabatic shear deformation for various strain rates.

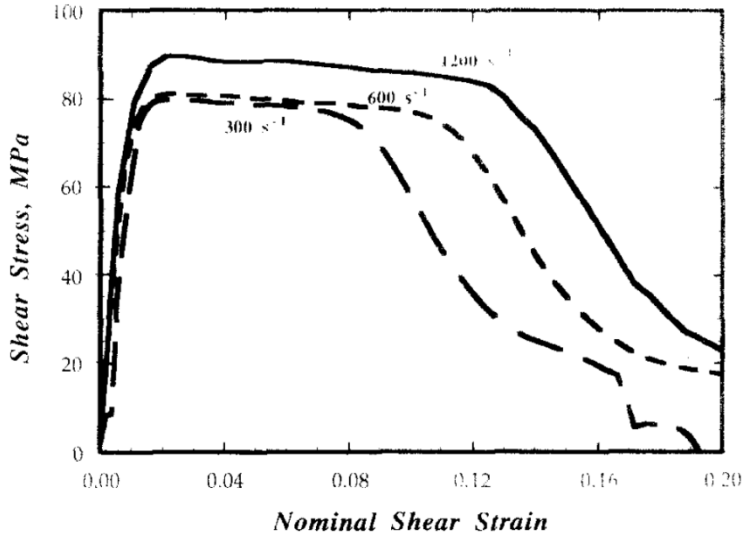

Figure 19 Shear stress vs. nominal shear strain showing adiabatic shear localization [49]

In the report published by German a more comprehensive study was done. The strain rate sensitivity of 90W-7Ni-3Fe at various test temperatures was reported. According to this report the stain rate sensitivity decreased as temperature increased. At 600^0C the alloy was no more strain sensitive, which is shown in Figure 20.

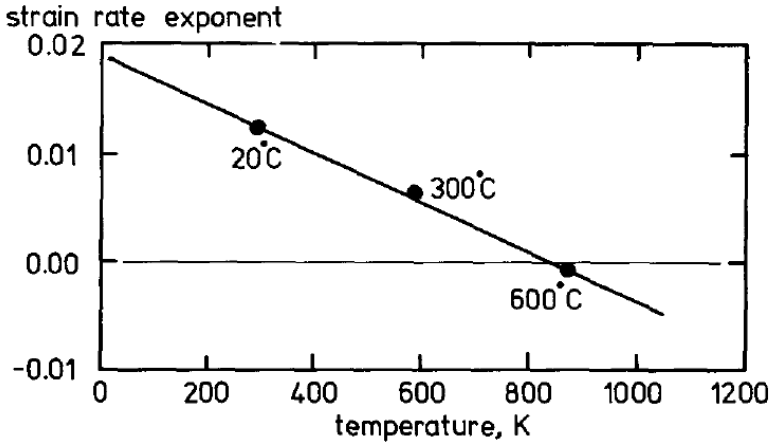

Figure 20 Strain rate sensitivity of 90-7-3 for various test temperatures [50]

The change of ductility with respect to the strain rate at various temperatures is shown in Figure 21.

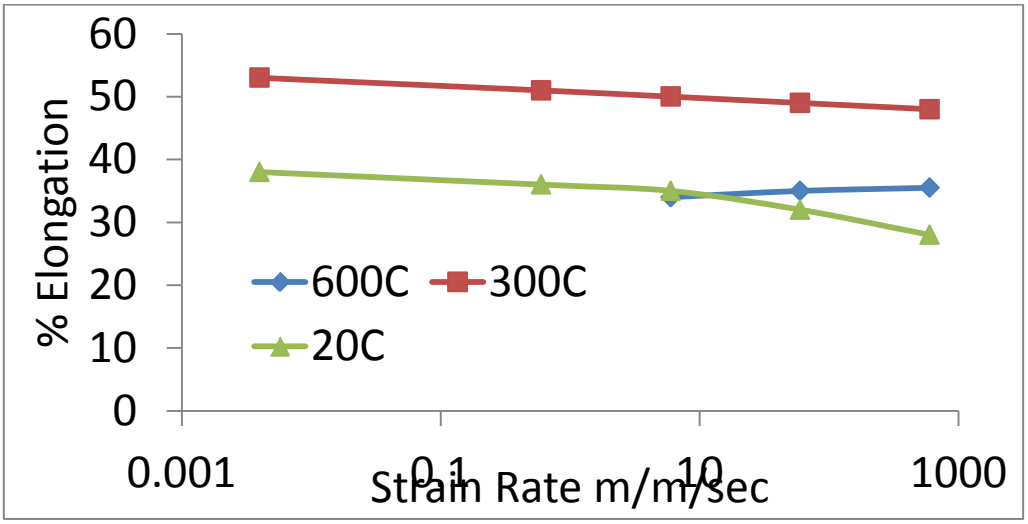

Figure 21 Variation of ductility with respect to cross head speed at various temperatures [49]

Also the changes in ductility and strength were reported. The strength decreased as the temperature increased, but the ductility had an asymmetric behavior as shown in Figure 22. The ductility was found to be the highest at 300C which is the same as reported for 95W-3.5Ni-1.5Fe alloy by Islam [51].

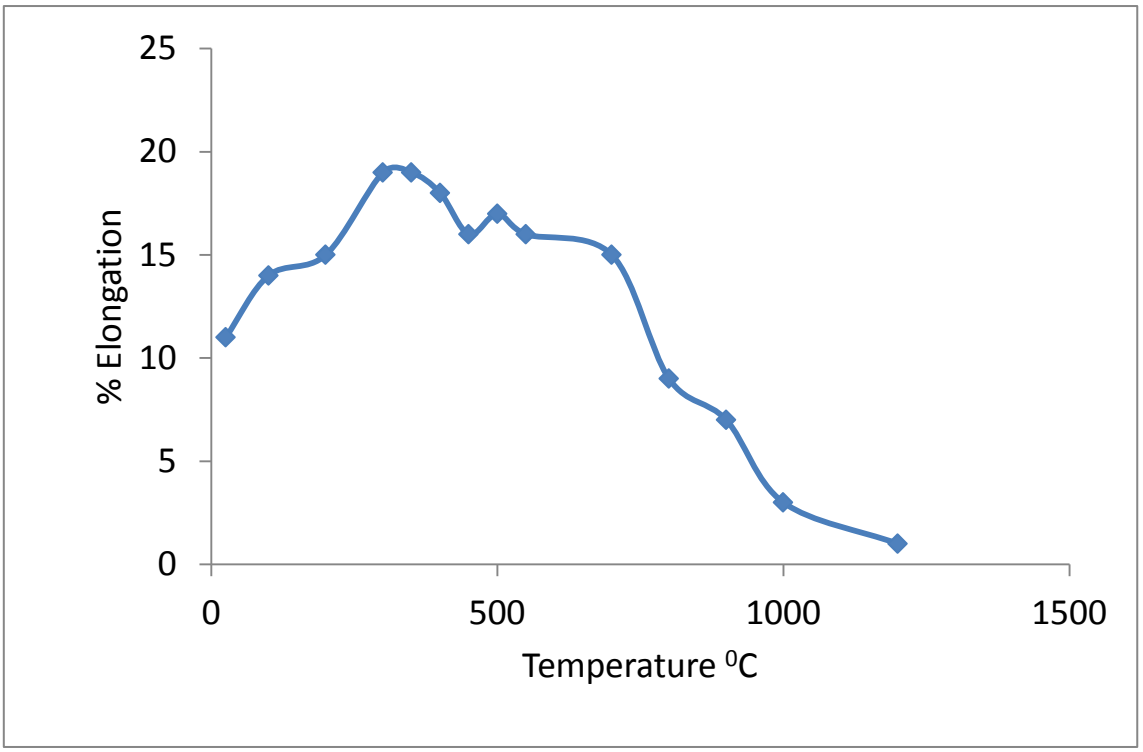

Figure 22 Change of ductility with increase in temperature of 95W-3.5Ni – 1.5 Ni [51]

Adiabatic Shear Banding

Adiabatic shear localization is a prevalent deformation and failure mechanism in materials which undergo high strain rates. Zerner and Hollman proposed the mechanism for adiabatic shear banding (ASB). It occurs when thermal softening overcomes the strain hardening. Ability to undergo ASB is important for self-sharpening behavior of a

material, which is used as a kinetic energy penetrator. Depleted uranium undergoes adiabatic shear banding at high strain rates, which are encountered during an impact with armor. Tungsten heavy alloy on the other hand has a tendency to undergo mushrooming.

Many studies have been done to improve the adiabatic shear banding ability of tungsten heavy alloys. Liu et al. subjected a tungsten heavy alloy (93W-4.5Ni-2.1 Fe-0.35Co) to both hot extrusion and hot torsion. The hot extrusion was done to elongate the tungsten grains (increase aspect ratio) and the hot torsion was performed to manipulate the angle between the elongated grains and loading direction. It was summarized that higher degree of hot torsion, higher the ability to shear localize. Highly localized shear bands were achieved when the tungsten grains were at 45^0 with the loading axis.

The same kind of result was also obtained by Wei et al. [52], in this report the influence of twist on shear banding was achieved on tungsten heavy alloy (93W-4.9Ni-2.1Fe). It was summarized that aspect ratio and orientation of grains with the loading axis is important in adiabatic shear banding of tungsten heavy alloy. Shear bands propagate easier when the major axis of the grains are parallel to the direction of shear stress. This is shown in Figure 23.

In many other efforts done to increase the susceptibility of tungsten heavy alloy, the matrix phase was replaced with materials which are known to undergo adiabatic shear banding. These materials include hafnium, high strength steel and titanium alloy. (Army p/m research and development review)

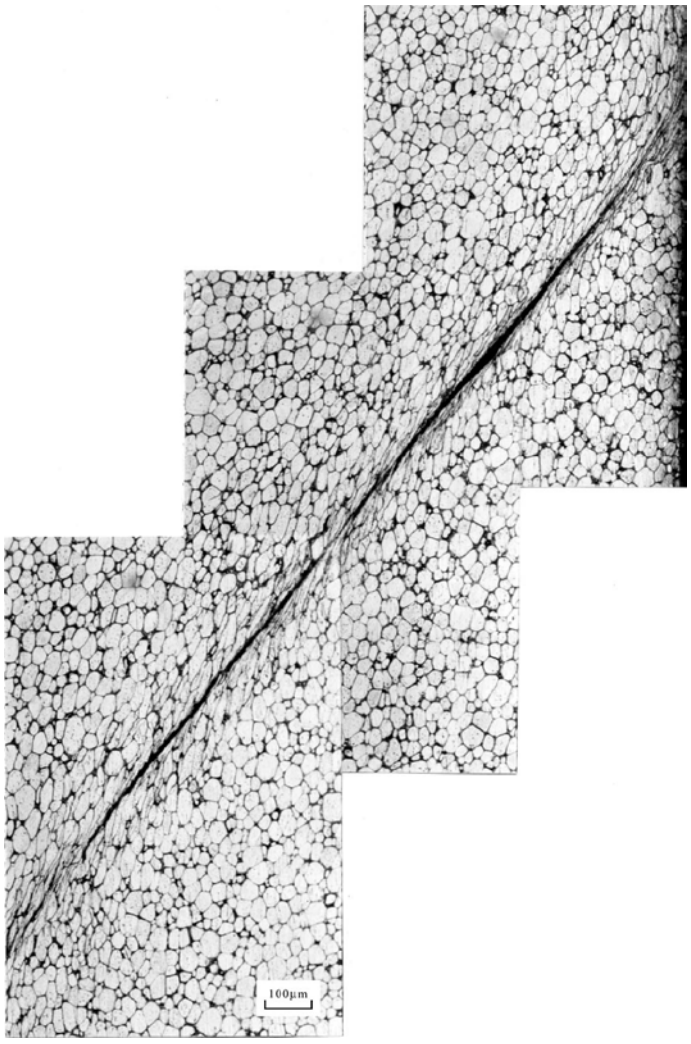

Figure 23 Shear band in tungsten heavy alloy [52]

EXPERIMENTAL PROCEDURES

Materials

The alloy used in our project is 90W-8Ni-2Fe, tungsten heavy alloy. This material was manufactured and shipped by our collaborators in Aeroject Tennessee. These billets were canned in type stainless steel containers to protect the tungsten heavy alloy from oxidation. The reasoning for choosing this material was discussed in previous sections. A schematic of billet to be extruded is shown in Figure 24.

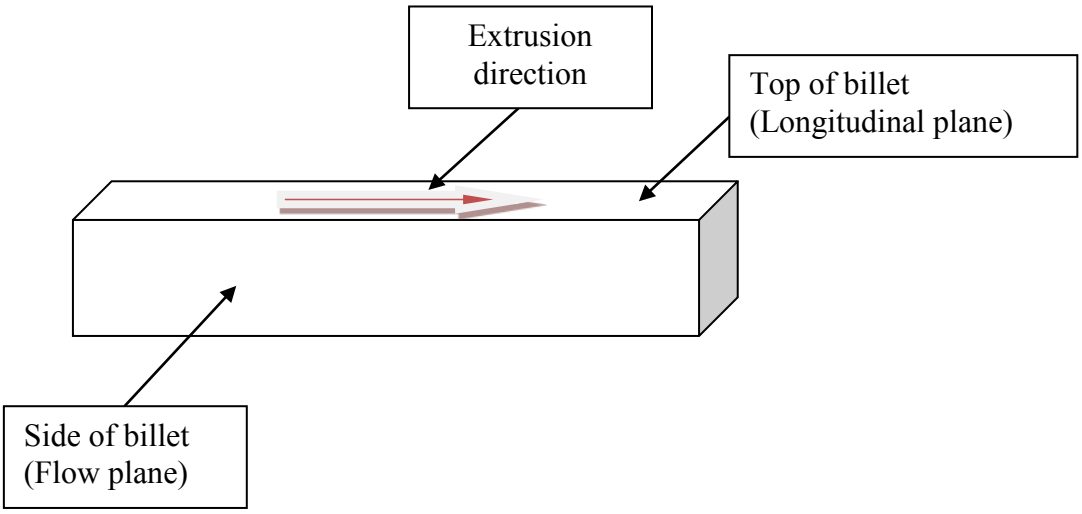

Figure 24 Schematic of a billet to be extruded

The schematic and the orientation of the billet after extrusion is given in Figure 25.

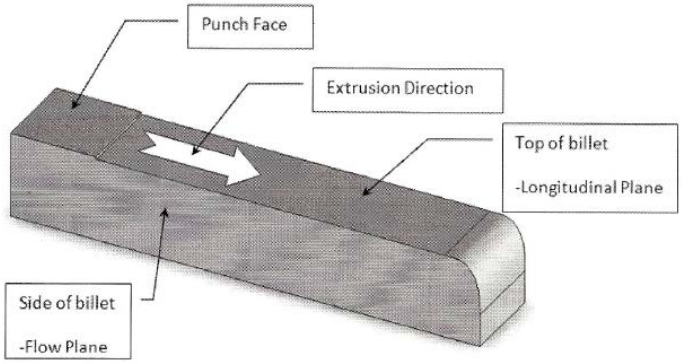

Figure 25 Schematic of a billet after extrusion

The chemical composition of the material used in this project is shown in Table 6.

Table 6 Elemental composition of tungsten heavy alloy used in this project

Element	Wt %
W	90
Ni	8
Fe	2

Processing

The ECAE processing was done at Texas A&M University, College Station. The die has its channels intersecting at 90^0 and has sliding walls. It was designed to take a maximum load of 260Kips. The die was designed by Mr. Robert Barber and Dr. Karl Hartwig. The press used was an MTS-controlled 225 ton hydraulic press. The starting material was

liquid phase sintered tungsten heavy alloy. Extrusions were done from temperatures of 300C – 1200C. The extrusions rates varied from 0.001in/sec to 1in/sec. The die was made from tool steel alloy which could be used up to temperatures of 300C. Also, the die used for these extrusions did not have any provision for applying back pressure.

Billets

The tungsten heavy alloy billets used in this project were manufactured using liquid phase sintering. These tungsten billets were canned in type stainless steel billets. The maximum wall thickness of the billets was about 0.125". The canning was done to avoid oxidation of tungsten when it encounters high temperatures during extrusion. The canning provides dynamic hydrostatic forces on the tungsten heavy alloy during the extrusion and also reduces cross-section area of the tungsten heavy alloy billet for extrusion. This decreased the load requirement to extrude. More often than not, the tungsten heavy alloy extrusion pushed the limits of the die, used for extrusion. The canning also helped to heat treat these billets after the extrusion for the next pass, without a need for an inert atmosphere.

The canned billets were machined to be nominally 1.00" by 1.00" in cross section. Initially the extrusions were done with 4" long billets to get an optimum processing technique. The final billets, i.e. the billets sent to Aerojet Tennessee were 5.5" long.

High Temperature Extrusions

High temperature extrusions were done in the temperature range of 800^0C to 1200^0C. The extrusion die is made of tool steel and the maximum safe use temperature of 300C.

The billet is heated in an oven separately to the required temperature. The extrusion rates of 0.5”/sec and 1”/sec, were selected such that isothermal conditions are maintained. The billet was coated with a glass colloid lubricant for these high temperature extrusions. Extrusions done at this temperature resulted in cracked and shear localized billets.

Low Temperature Extrusions

The low temperature extrusions were done at 300^0C, because tungsten alloys were reported to have maximum ductility at this temperature. The extrusion was done at very slow speed. Successful extrusions were possible at an extrusion rate of 0.003 in/sec. The billets were lubricated with an anti-seize. The billets were heated in the die, for half an hour before the start of extrusion, this is pre-heating. This was done to make sure that the billet was at 300C during extrusion.

After the extrusion the billet was quenched in water. The quenching was done for both, the high temperature and low temperature extrusions.

Thermal Processing for Multiple Passes

No heat treatment was done on the as-received billets before the first pass. When a second pass was attempted, without any intermediate annealing, the billets shear localized during the extrusion. To successfully achieve a second pass, an intermediate annealing was done on these billets. The billets which were processed 1A were annealed at 1300C for one hour. If the material was to be processed for the third pass, the annealing was done after both the first and second passes. The stainless steel cans protected the tungsten heavy alloy from oxidation during annealing.

Challenges Faced

The extrusions were challenging during the initial stage of the project. Because of not much literature was available on extrusion of these alloys, the processing parameters like the extrusion temperature and extrusion rate were determined by trial and error. Many billets fractured and shear localized before we could identify feasible processing parameters for successful extrusions. We had success in extruding these materials at 300C at a maximum extrusion rate of 0.003 in/sec. Processing by route C, with intermediate annealing proved successful for the second pass. The third pass was processed via route E. The billet was turned 90^0 after the 2C pass. Attempts with the 120^0 die were unsuccessful. The billets shear localized.

After processing samples were cut from the central portion of the billet with a diamond saw for characterization studies.

Recrystallization

Samples of 0.25”X0.25”X0.5”were cut using a diamond saw, for examining the recrystallization behavior. These samples were sealed in quartz under a vacuum of at least 10^{-4}torr. These samples were annealed in a furnace for about 1 hour at the required temperature, and quenched. The samples were heated at the following temperatures: 300^0C, 500^0C, 700^0C, 900^0C, 1100^0C, 1200^0C and 1300^0C. After these samples were heat-treated they were cut into half and measured for hardness using the Rockwell C scale. The cutting was done using a diamond saw at slow speeds. It was done to avoid

any data dilution, due to oxidation or unforeseen effects. These samples were also examined for their microstructure in optical and scanning electron microscope.

Characterization

The characterizations used in this project were

- Microscopy
    - Optical
    - Scanning electron
- XRD
- Hardness
    - Rockwell hardness

X-Ray Diffraction

Samples of 0.8 x 0.8 x 0.05 inch in dimensions were cut using a diamond saw for x-ray diffraction analysis. The sample was polished to 1200 grit. Care was taken to make sure that no particulate matter was present on the surface, on which XRD was performed. A short-arm Bruker-AXS D8, with a copper source at 40KV and 40mA was used to collect the XRD data. The beam was 1mm wide.

The samples were mounted on a disk such that the surface to examine is flat with respect to the reference of the machine. Craft putty was used to mount the samples on the disk. The same setup was used for all the samples. Typically the range of the angles examined covered from 35 – 90 degrees with a 0.1degree/sec scan rate.

Microscopy

Sample Preparation

The samples were prepared in similar fashion for both optical and scanning electron microscopy. The samples were cut from the central portion of the billets and mounted in Bakelite. The mounted billets were polished using a Strauss polisher. The polishing procedures were followed as suggested by buheler. Care was taken to make sure the surface was flat and free from scratches. The two sides of the sample were made parallel.

For SEM imaging of the WHA samples, the samples were made conductive by using aluminum foil and double side carbon tape. The size of the Bakelite mount was selected such that it matches the size of the SEM holder. The aluminum foil covered the whole of the mount with holes for the areas which are imaged. The foil was attached to the Bakelite using carbon tape. One side of the carbon tape was attached to the metal piece which was being imaged; the other side was attached to the aluminum foil. The foil acts as a ground for the electrons which hit the sample from the e-beam.

Hardness Measurements

Hardness was measured on as-received, ECAE processed and recrystallized samples. The hardness measurements were done by using a Rockwell Hardness Machine.

The samples for Rockwell hardness testing were cut from the areas of the billets which are fully processed to the required conditions. These samples were cut such that they had parallel surfaces. The side, on which hardness measurements were taken, was polished to

600 grit. Then these surfaces were cleaned to ensure particulate free surface, which could compromise the reliability of the data.

The machine was checked for its accuracy using a calibration sample. Rockwell C scale was used for all the measurements. Five measurements were taken for each sample. The mean, standard deviation and other statistical data were also obtained from the machine itself.

EXPERIMENTAL RESULTS

ECAE Processing

The tungsten heavy alloy billets of 1”x 1” were extruded through a 90 degree die. All the extrusions were done without any back pressure. These materials are strain sensitive, even at higher temperatures i.e. at greater than 800C these materials shear localized at extrusions rates of 0.5 “/sec and 1 “/sec. High speed was necessary to maintain isothermal conditions. Figure 26 shows an un-canned shear localized billet.

Figure 26 Shear localized WHA billet extruded at 1200C at 0.5"/sec

Shear localization can be identified in the load-stroke curve as a discontinuity in the curve. This allows us to identify if any shear localization is occurring during the course of the extrusion. The load stroke curve of a shear localized billet is shown in Figure 27. For all temperatures at and between 800C and 1300C these materials shear localized at 0.5”/sec extrusion speed.

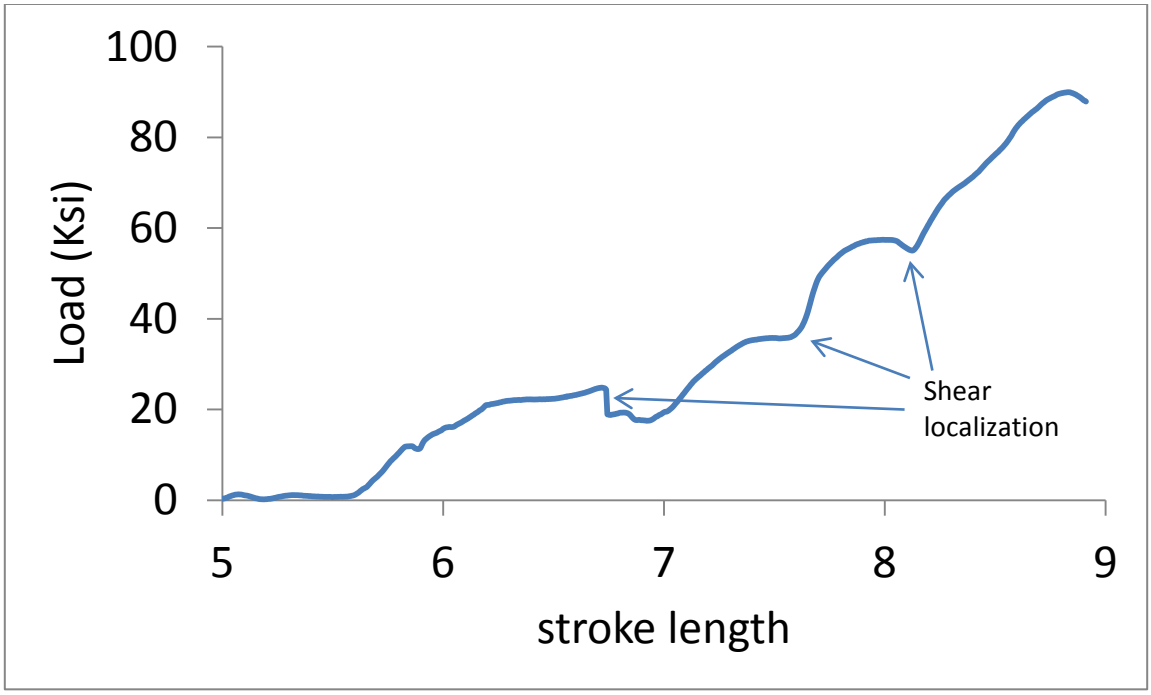

Figure 27 Stroke - load curve of W2 billet processed at 1200C and 0.5"/sec

Successful extrusions were accomplished at 300C and low extrusions rates of 0.001”/sec and 0.003”/sec. These extrusion conditions allowed us to process billets without fracture.

The ECAE loads were measured during the extrusions. Table 7 shows maximum loads during extrusion of tungsten heavy alloy billets. The data presented is for extrusions done at 3000C and at an extrusion rate of 0.003”/sec. These conditions were found to be sufficient for processing the WHA material. In fact these conditions were the only successful extrusions.

Table 7 Maximum loads encountered during extrusion via 1A, 2C and 3E routes

Route	Avg Max Load (Kips)	Lowest max load (Kips)	Highest Max load (Kips)	Std deviation
1A	236	206	255	17.3
2C	194	187	204	7.4
3E	233	233	233	0

A load curvesfor1A, 2C and 3E processed tungsten heavy alloy is shown in Figure 28.

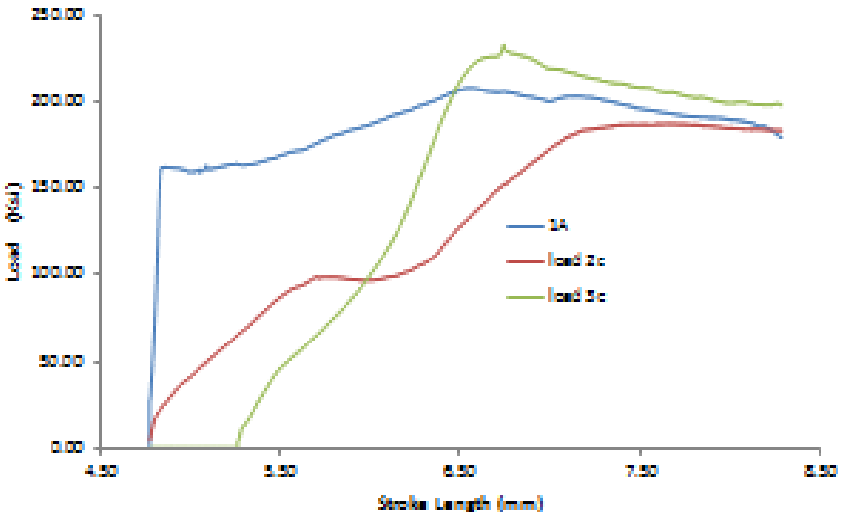

Figure 28 Load stroke curve of 1A, 2C and 3E passes of a WHA billet

During the first extrusion the as received sample was extruded without any heat treatment. These extrusions were done near the load limit of the die. The average maximum load during the first pass was 236 kips, with a highest load of 255kips. Sometimes the load limit crossed 255 kips at which point the extrusions was stopped and the billet was ejected.

For the second pass via Route C the 1A processed billet was annealed for one hour at 1300C and furnace cooled. These annealed billets did not fail during the second pass as the ones without any intermediate heat treatment did. The billets which were processed after heat treatment came out in good shape and were ready to be processed for one more pass. The average maximum load on this pass was 194 kips, which is 42 kips below the average for the first pass. The difference between the first and second pass is so prominent that the highest maximum load on the second pass (2C) was lower than the lowest max load on the first. This is typical extrusions via route C.

Only one billet was processed for a third pass and the maximum load during extrusion on this one was 233 kips which is approximately same as the average for first pass. For the third pass the billet was rotated 90^0 and extruded to achieve uniformity.

The maximum loads for each pass and their standard deviations are shown in Figure 29.

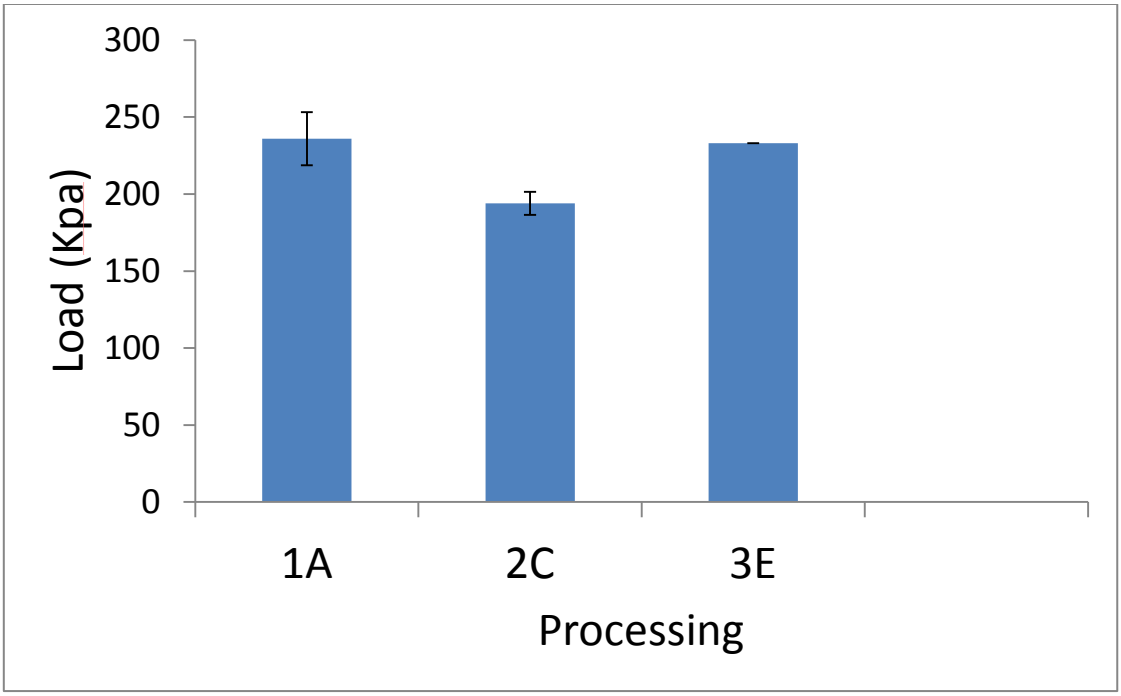

Figure 29 Maximum loads with their standard deviation for 1A 2C and 3E passes

Microstructure

The microstructures of ECAE processed tungsten heavy alloy were examined using both an optical and scanning electron microscope. The use of a scanning electron microscope did not reveal any extra details but helped to take a closer look at the interface between the tungsten particles and nickel-iron alloy phase. The microstructures were examined on the flow plane. Prior to microscopic examination, the samples were polished and etched as mentioned in the procedures section. The size and aspect ratios of tungsten particles are presented in Table 8.

Table 8 Size, shape and other properties of tungsten heavy alloy microstructure

Processing Route	Tungsten Particle Size	Average Length of major axis (μm)	Average Length of minor axis (μm)	Aspect Ratio
As-received	Spherical	22	22	1
1A	Elliptical	50.5	10.1	5.2

The microstructures of as received tungsten heavy alloy samples of different magnification are shown from Figure 30 to Figure 32. The average diameter of the tungsten grains is 22 μm with a standard deviation of about 8.6μm. The minimum and the maximum diameters of the tungsten particles are 7.2 and 45.5 μm. Some diffusion bonding between the tungsten particles observed.

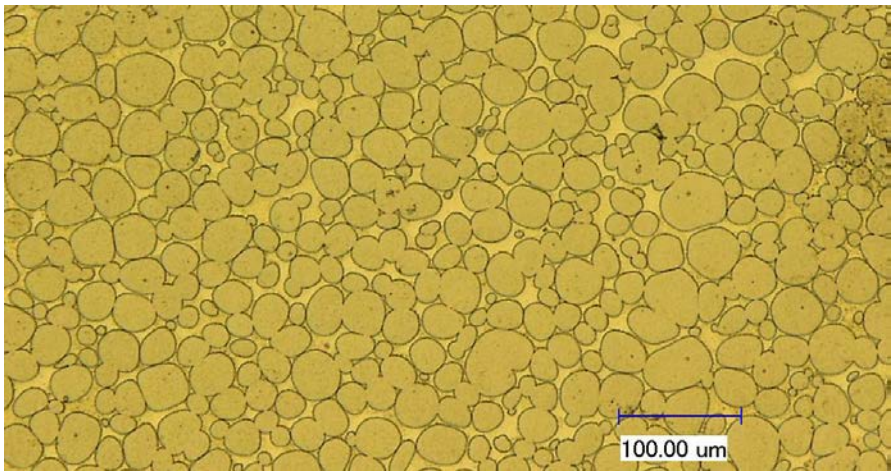

Figure 30 Microstructure of as-received tungsten heavy alloy at 300X magnification

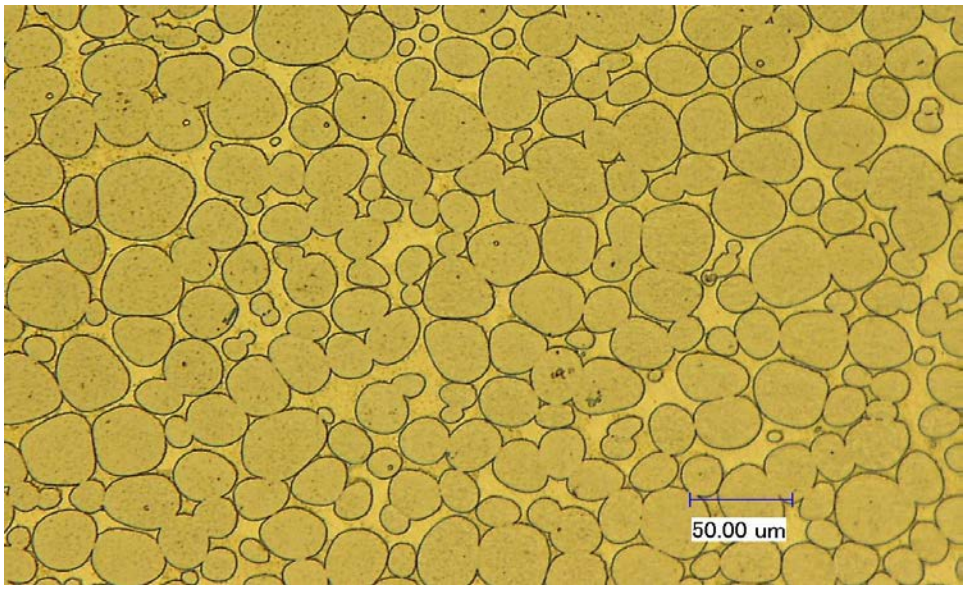

Figure 31 Microstructure of as-received tungsten heavy alloy at 500X magnification

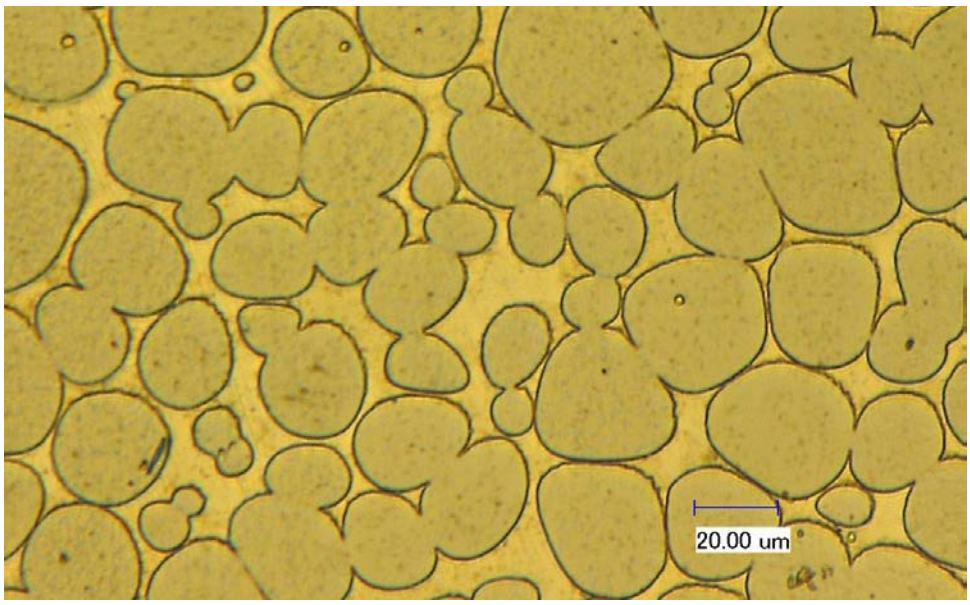

Figure 32 Microstructure of as-received tungsten heavy alloy at 1000X magnification

The scanning electron microscope images of the same are shown in Figure 33 and Figure 34 . The interface between the tungsten particles and the alloy matrix is smooth. This is typical for liquid phase sintered tungsten heavy alloys.

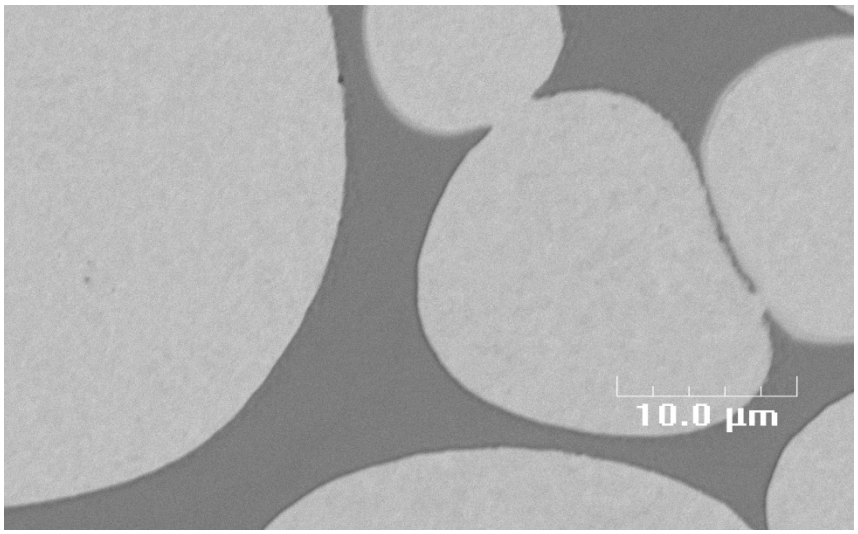

Figure 33 Backscattered image of as-received tungsten heavy alloy at 2000X

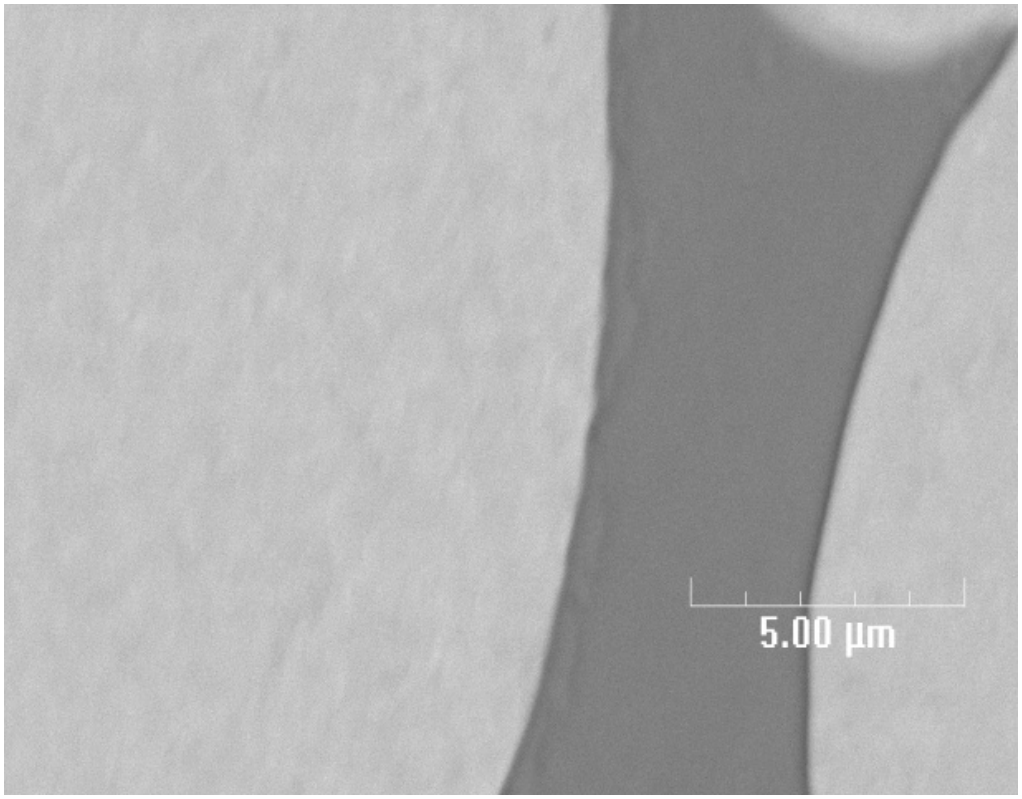

Figure 34 Backscattered image of as-received tungsten heavy alloy at 6000X

First Pass (Route A)

The microstructures of single pass ECAE billets at 300C and 0.003”/sec extrusion rate are show below. These microstructures were examined in an optical microscope. Figure 35 to Figure 37 show the microstructure of single pass processed tungsten heavy alloy at various magnifications. The dimensions and aspect ratios of the tungsten particles in these samples were measured assuming an elliptical shape for the tungsten particles. The aspect ratios of these grains averaged at 5.20 with a standard deviation of 1.95. The

minimum and maximum aspect ratios are 10 and 2. The average lengths of major and minor axis with their standard deviations are 50.5 +/- 25 and 10.1 +/- 4.5 µm.

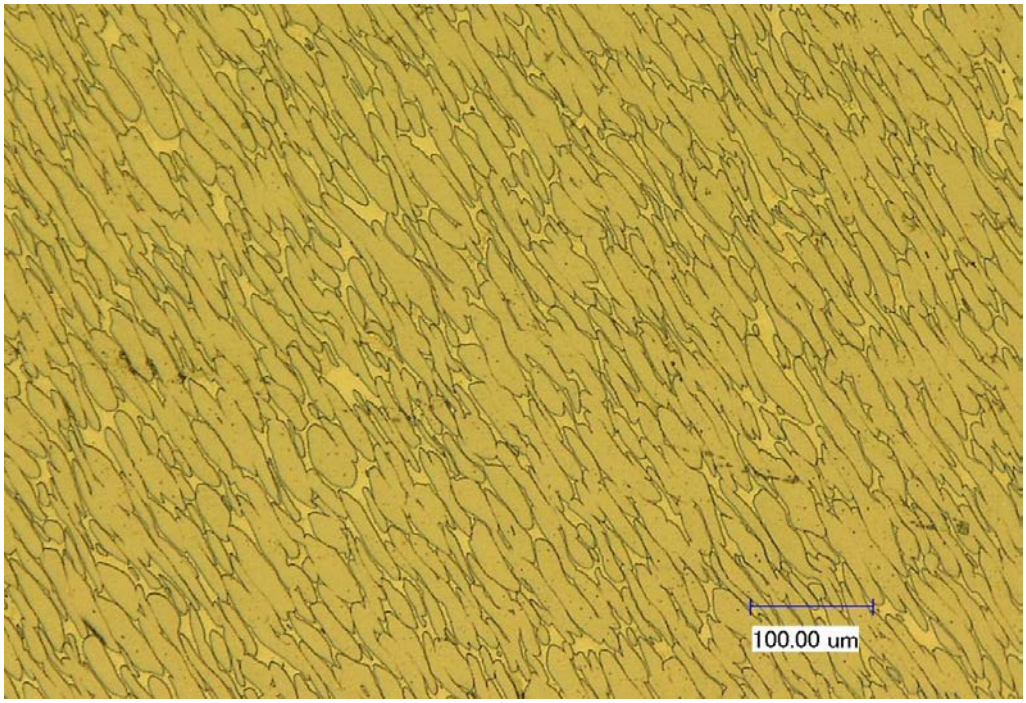

Figure 35 Microstructure of single pass ECAE tungsten heavy alloy at 300X magnification

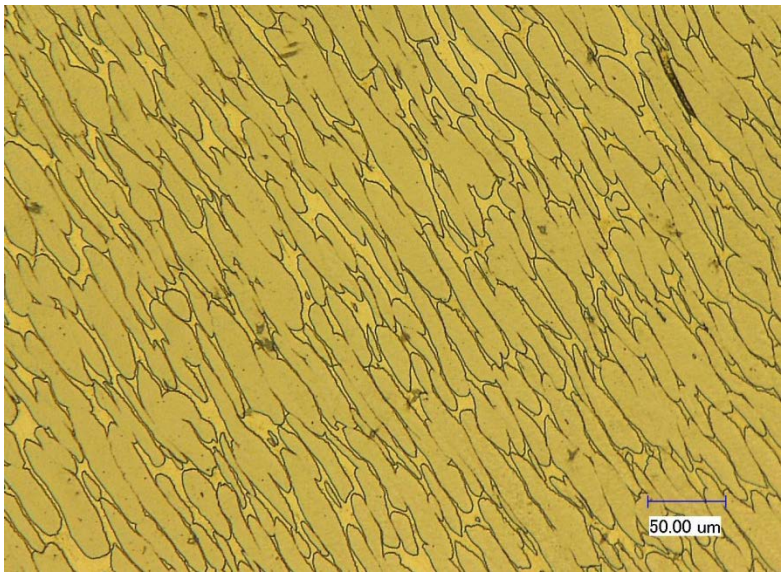

Figure 36 Microstructure of single pass ECAE tungsten heavy alloy at 500X magnification

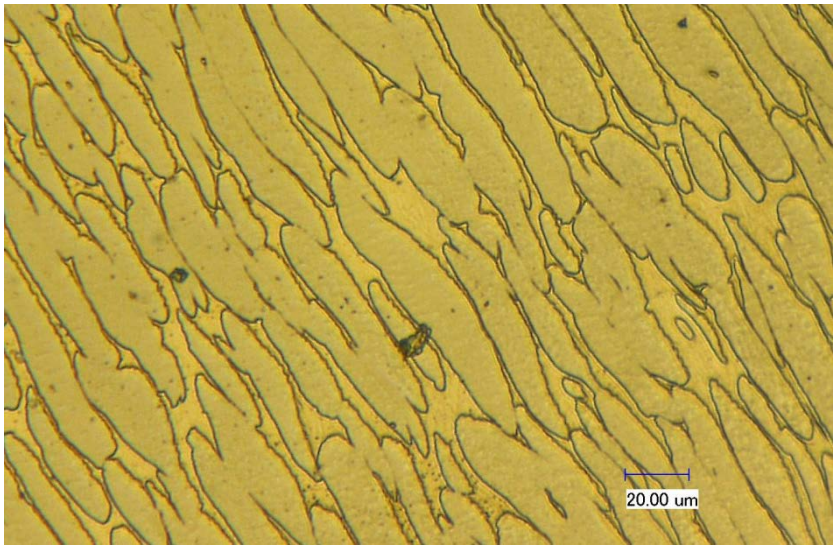

Figure 37 Microstructure of single pass ECAE tungsten heavy alloy at 1000X magnification

The back scattered images of tungsten heavy alloy after single pass extrusion is shown in Figure 38 and Figure 39 . We see some roughness between the tungsten particle and alloy matrix interface.

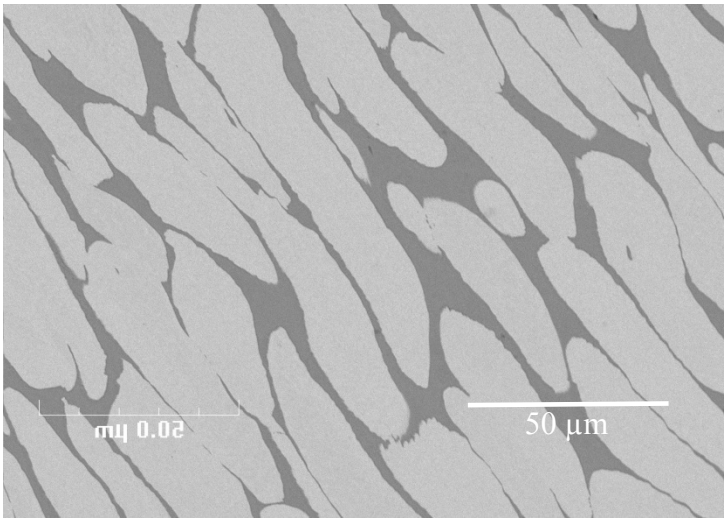

Figure 38 Backscattered image of 1A processed tungsten heavy alloy at 2000X

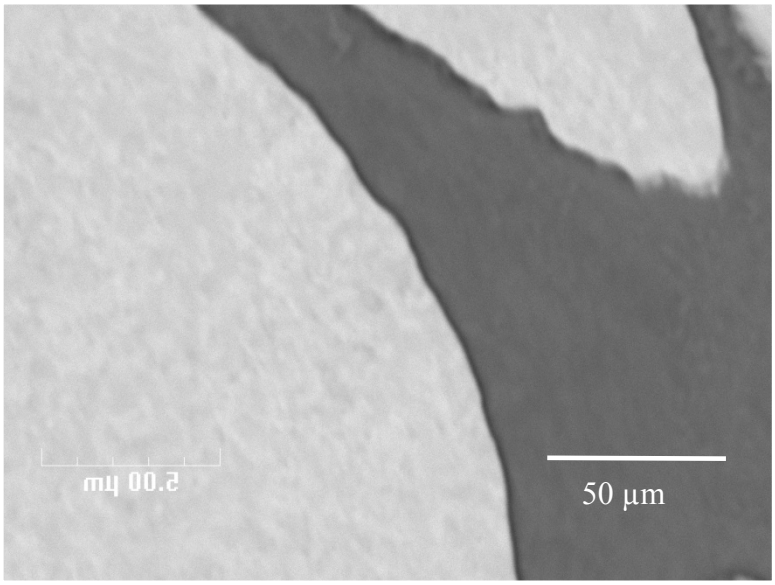

Figure 39 Backscattered image of 1A processed tungsten heavy alloy at 6000X

Second Pass (Route C)

The second pass on the billets was done via the C route. These billets were annealed at 1300C for one hour and furnace cooled to room temperature before the second pass. The extrusions were done at 300C and at an extrusion rate of 0.003”/sec, with no back pressure.

The microstructures of these samples are shown from Figure 40 to Figure 42 at various magnifications.

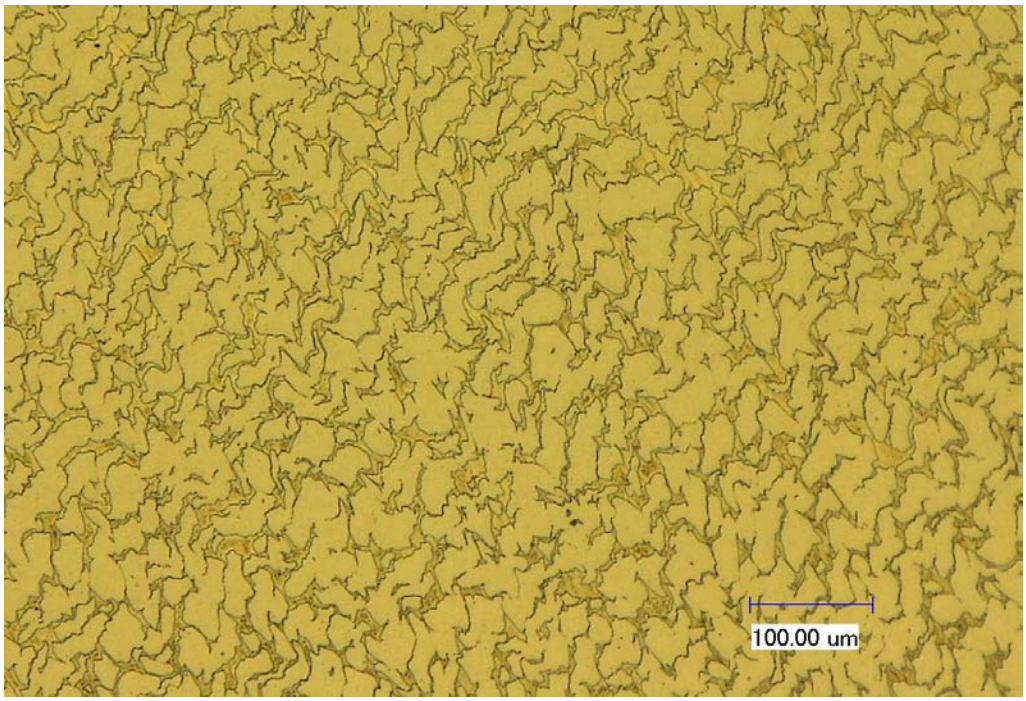

Figure 40 Microstructure of 2C processed WHA at 300X magnification

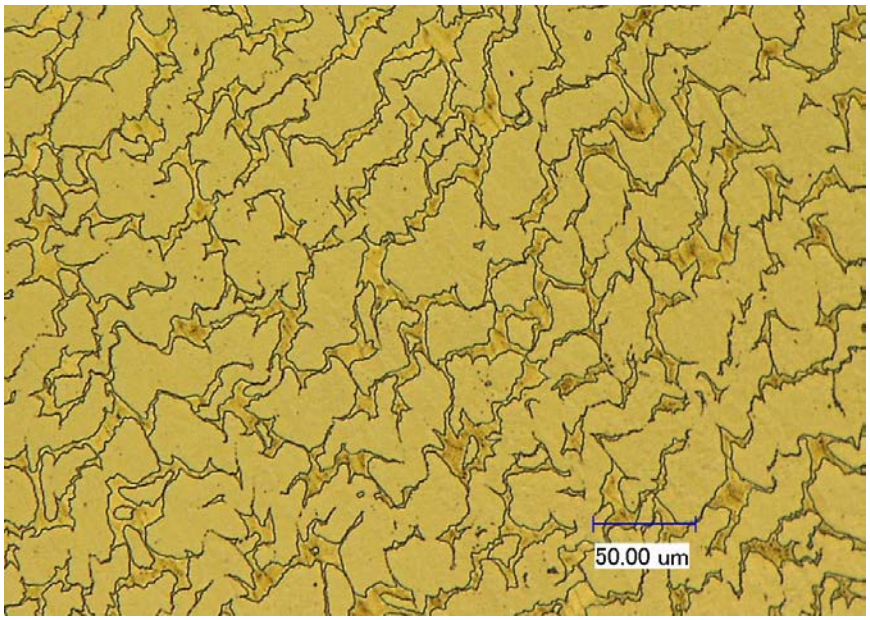

Figure 41 Microstructure of 2C processed WHA at 500X magnification

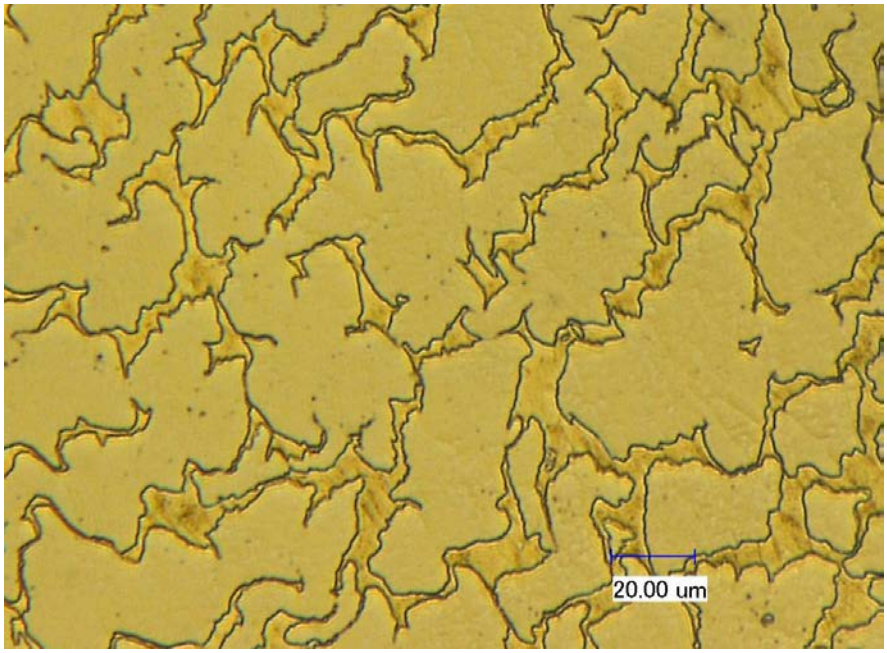

Figure 42 Microstructure of 2C processed WHA at 1000X magnification

The microstructure obtained after 2C processing was scrambled and was termed "popcorn microstructure". No such microstructure was reported in the literature till now. The backscattered scanning electron microscope image is shown in Figure 43.

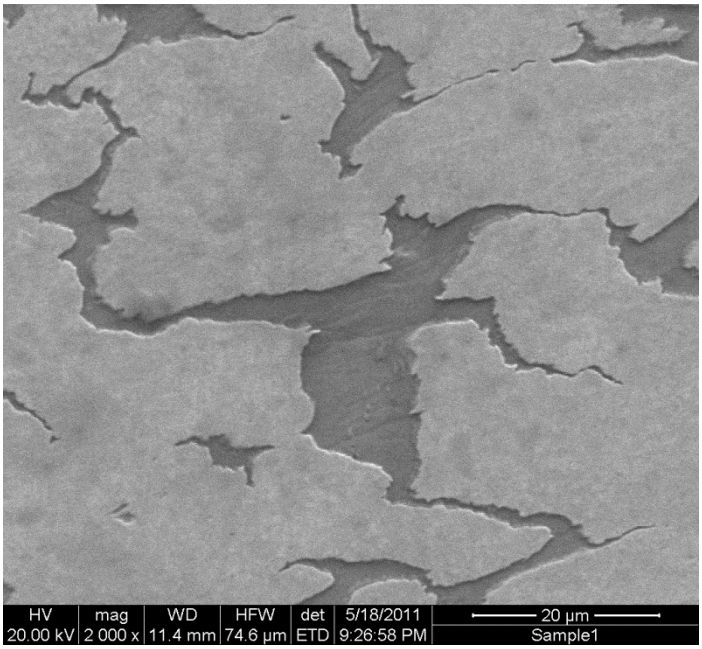

Figure 43Backscattered image of 2C processed WHA at 2000X

Third Pass

The third pass was done via route E. The 2C processed sample was annealed at 1300C for one hour and furnace cooled. The processing conditions for 3E route were same as for 2C route. The microstructure obtained has elongated grains. It was similar to the microstructure obtained after the first pass, but the interface between the tungsten particles and nickel-iron alloy interface is rough. Optical microscopy images are shown from Figure 44 to Figure 46.

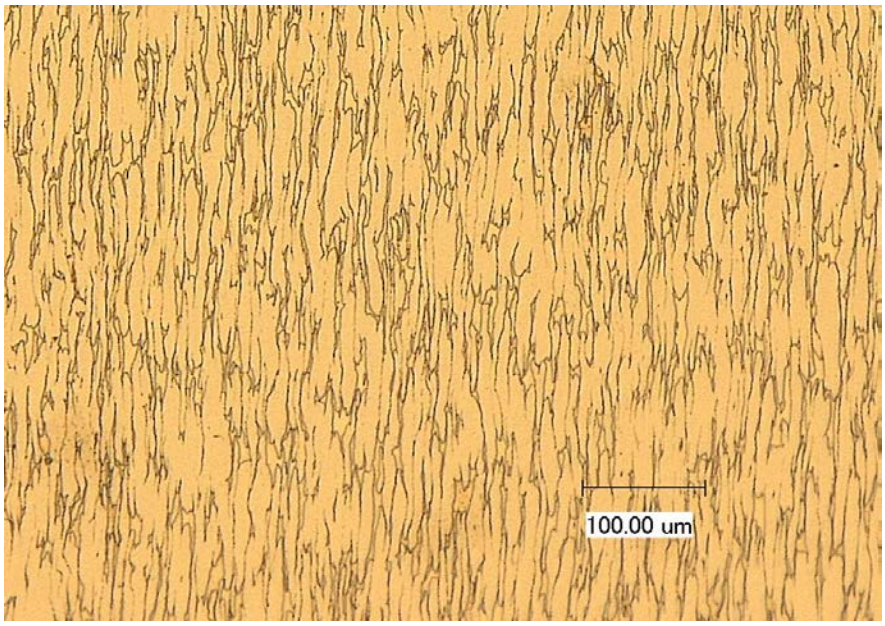

Figure 44 Microstructure of 3E processed WHA at 300X magnification

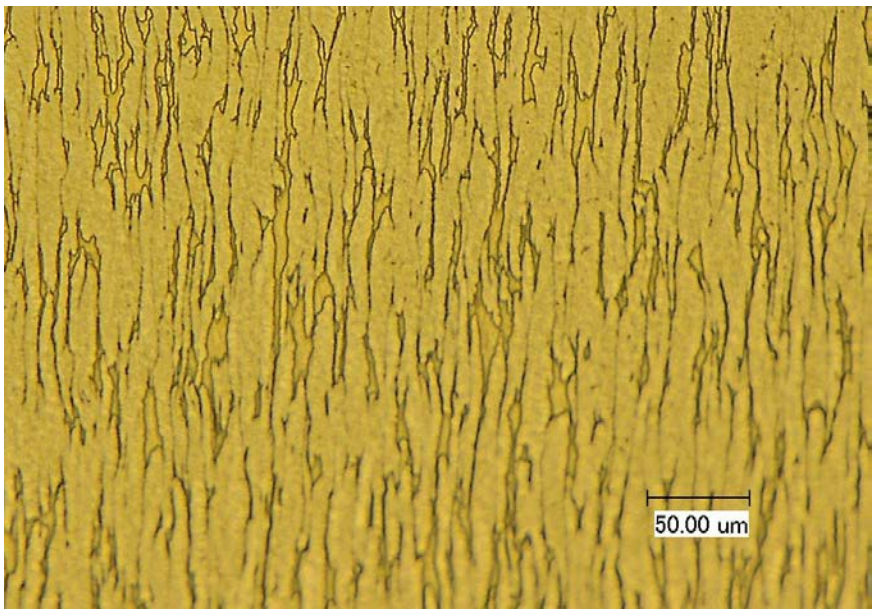

Figure 45 Microstructure of 3E processed WHA at 500X magnification

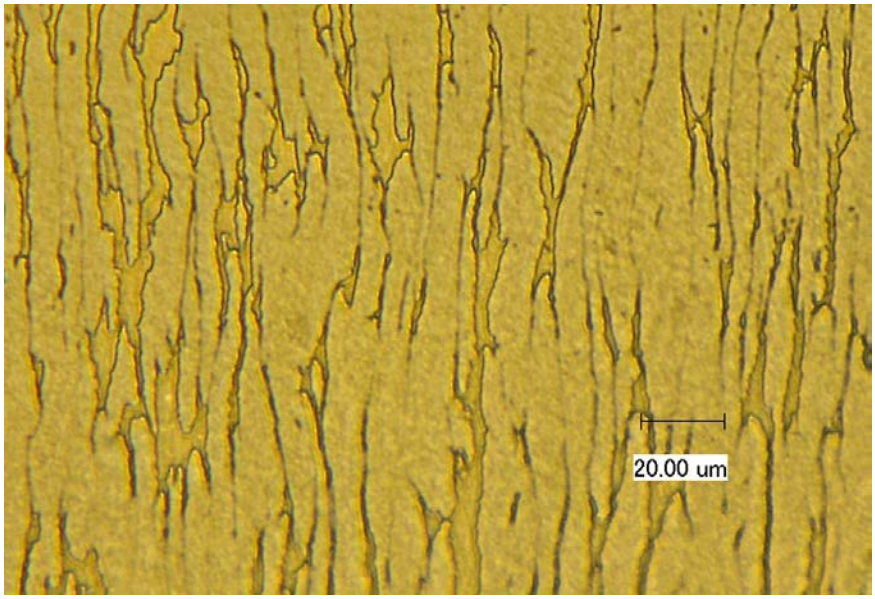

Figure 46 Microstructure of 3E processed WHA at 1000X magnification

Higher magnification images of the same microstructure are shown in Figure 47 and Figure 48.

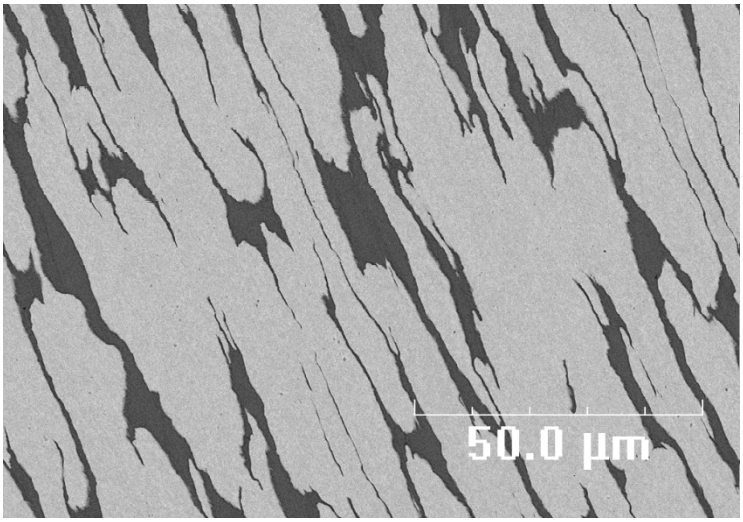

Figure 47 Backscattered image of 3E processed WHA at 2000X

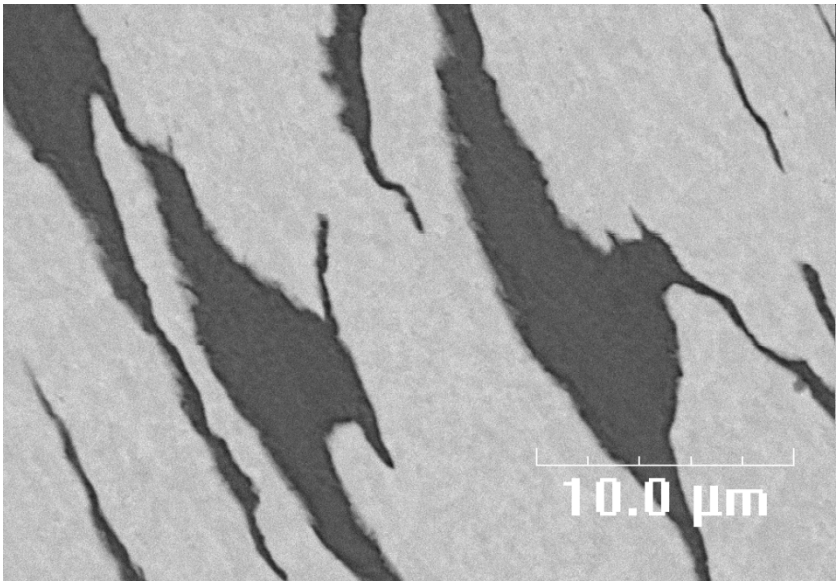

Figure 48 Backscattered image of 3E processed WHA at 2000X

X-Ray Diffraction

XRD was performed on 1A, 2C and 3E processed samples. Also the analysis was done on as received, 1300C annealed, 700C annealed and as-received annealed samples. The tungsten,, iron and nickel peaks are identified from powder diffraction standards and the d spacing in the literature. As it can be seen in Figure 49**,** the phases are the same in all the three cases of heat treatment. No appreciable change is found in the peak location, their height, or their width. The wolfram (W) phase with peaks of (100), (200), (211) and (220) are identified at 40^0, 58^0, 73^0 and 86^0. Their peak heights are different. Also the Ni, Fe solution phase is also identified with peaks of (111), (200) and (220) at 43.5^0, 53^0 and 74^0. The relative peak heights of both the wolfram and the Ni-Fe solution phase decreasing in the order mentioned. This can be expected as ECAE processing imparts texture to the material.

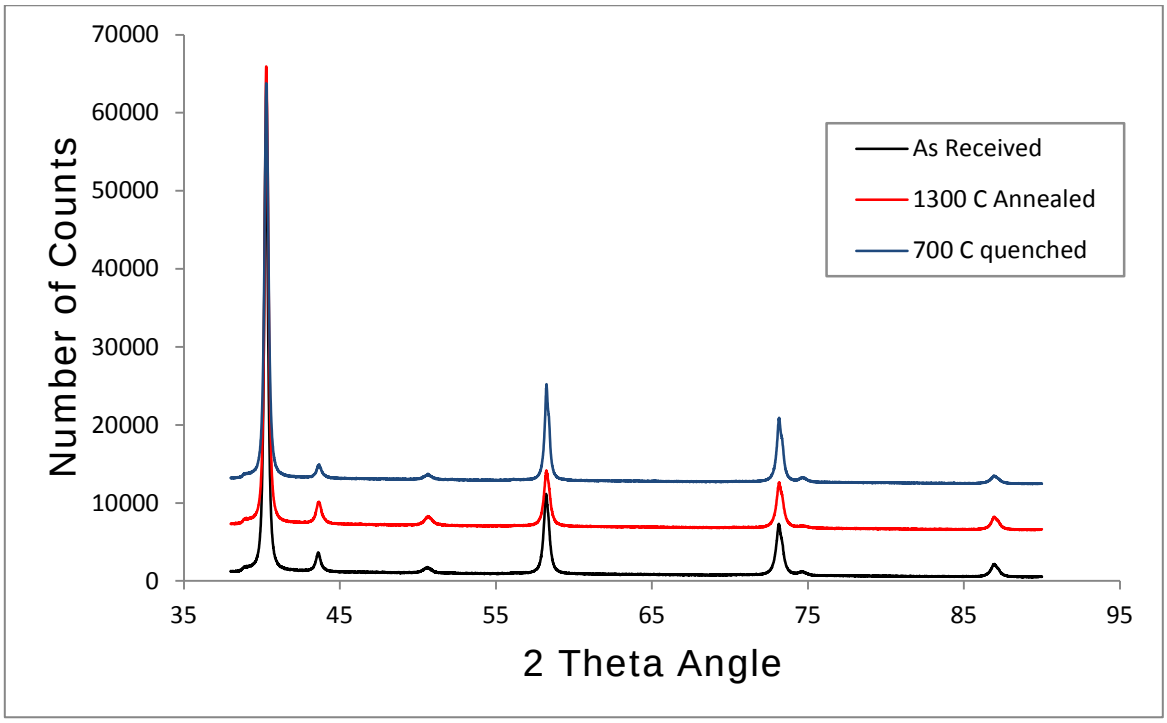

Figure 49 XRD analysis of as-received, 700C and 1300C quenched samples

Hardness

The hardness of ECAE processed WHA billets were measured using the Rockwell C scale. Material was selected from an area of the billet which represents the total processing done on it. The testing was done on a standard Rockwell testing machine as mentioned in the previous section. The hardness of as received and ECAE processed WHA billets are shown in Table 9.

Table 9 Rockwell hardness of as received and ECAE processed tungsten heavy alloy

Processing	Hardness (HRC)	Std deviation
As received	23.6	2.5
1A processed	47.4	0.2
1A + 1300C annealed + 180^0 1A = 2C	45.1	0.6
1A + 1300C annealed + 180^0 1A + 1300C annealed +901A = 3E	47.3	0.2

Hardness data is graphically represented in Figure 50. The hardness of as-received material was around 23.6 HRC. After the first extrusion of the as-received tungsten alloy the hardness increased to 47.4 HRC. For the second pass the billet was annealed at 1300C and processed for the next pass. The hardness of the 2C processed material is around 45.1 HRC which is nearly same hardness as the first pass billet. The hardness during the third pass is around 47.3 HRC.

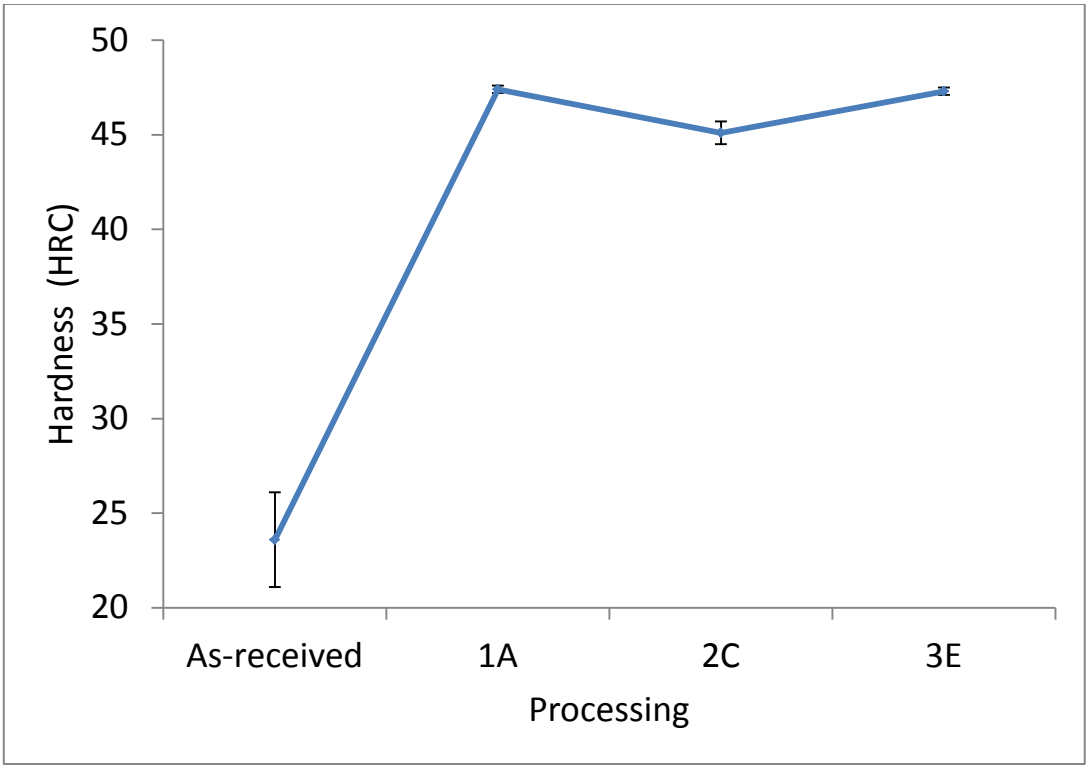

Figure 50 Rockwell hardness of as-received and ECAE processed WHA

Recrystallization Behavior

The recrystallization behavior of 1A processed WHA was measured using the Rockwell hardness scale. Samples were cut from 1A processed material. These samples were sealed in evacuated quartz tubes and heat treated for one hour at the stated temperatures. Samples were heat treated at 300^0C, 500^0C, 700^0C, 900^0C, 1100^0C, 1200^0C and 1300^0C. Hardness and microscopic measurements were done on heat treated samples. The hardness data is shown in Table 10.

Table 10 Recrystallization behavior of 1A processed WHA alloy

Temperature (^{0}C)	Hardness (HRC)	Standard Deviation
25	47.6	0.2
300	47.3	0.26
500	49.46	0.30
700	47.78	0.90
900	44.12	0.80
1100	32.76	1.74
1200	31.725	0.51
1300	32.24	0.41

The recrystallization curve of 1A processed billet is shown in Figure 51. The figure shows a modest increase in hardness from 47.3 to 49.4 HRC in the temperature range of 300 to 500^{0}C. A modest softening from 49.4 to 44.2 HRC is seen, beginning at about 500C to 900C. An increased softening rate is seen beginning at about 900^{0}C, and a leveling off at about 1100^{0}C to a hardness of about 32 HRC.

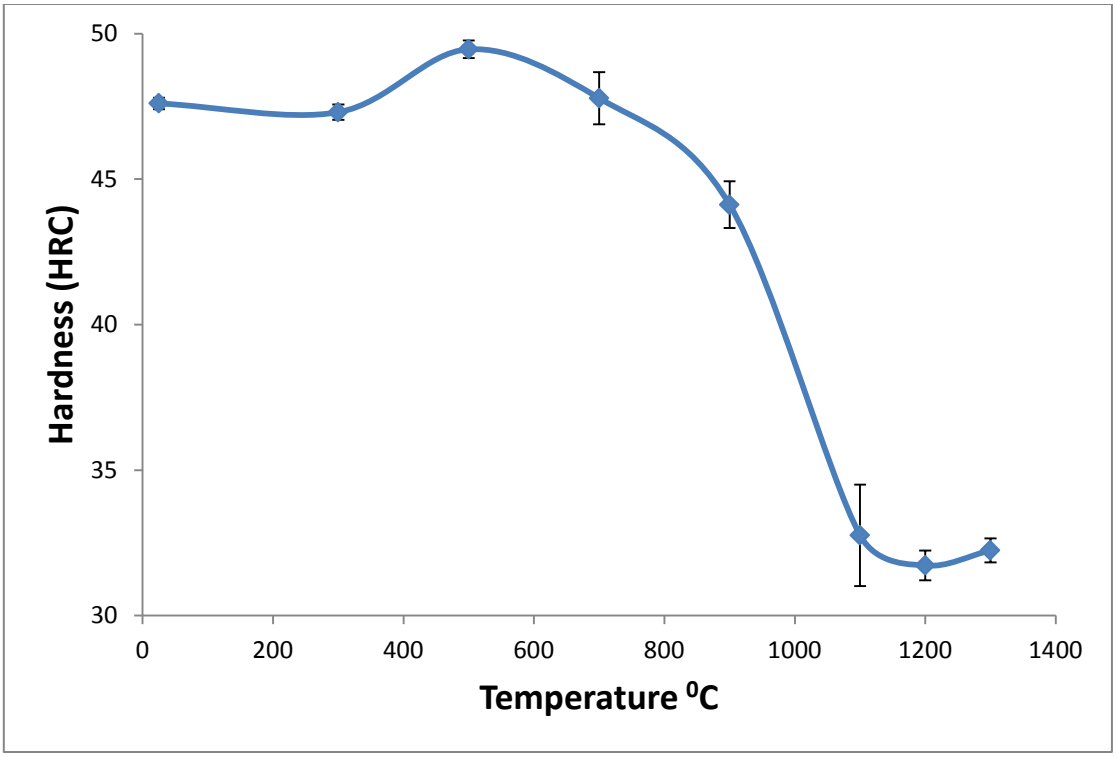

Figure 51 Recrystallization curve of 1A processed tungsten heavy alloy

Microstructure of Recrystallization Samples

The microstructures of the recrystallized samples were examined. The samples after heat treatment were cut into half to expose internal material for examination. One sample was used for measuring the Rockwell hardness; the other sample was polished and etched using 3ml HF + 15ml HNO_3+ 80ml H_2O. The microstructures of recrystallized samples are shown in the following figures. Figure 52 shows the microstructure of a 1A processed WHA alloy, heat treated at 300^0C. The hardness of this sample after heat treatment is 47.3HRC, which is same as the one at room temperature.

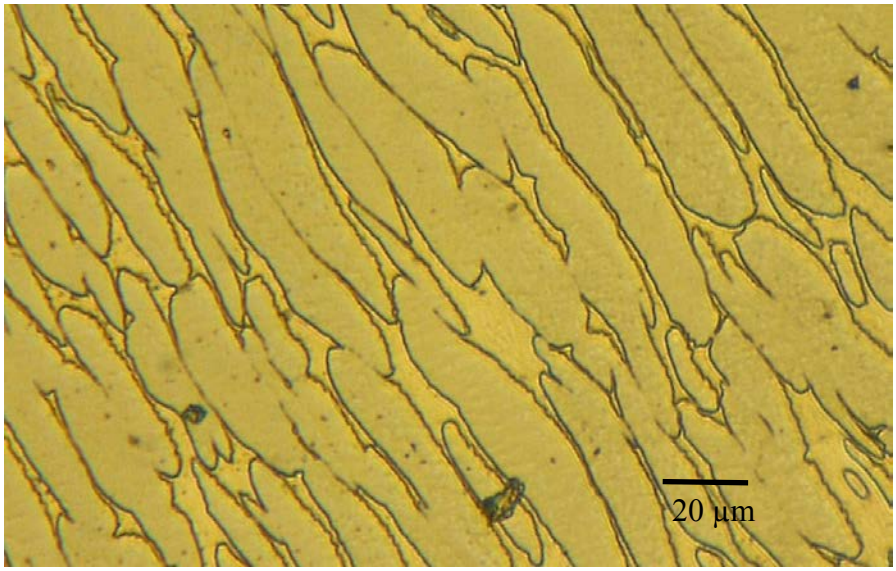

Figure 52 Microstructure of 1A processed WHA heat treated at 300^{0}C

Figure 53 shows the microstructure of the same 1A processed sample, which is heat treated at 500C. The hardness of this sample is 49.5 HRC which is higher than the one at room temperature (RT) and 300C. The microstructure of this sample is not significantly different from the RT and 300C samples.

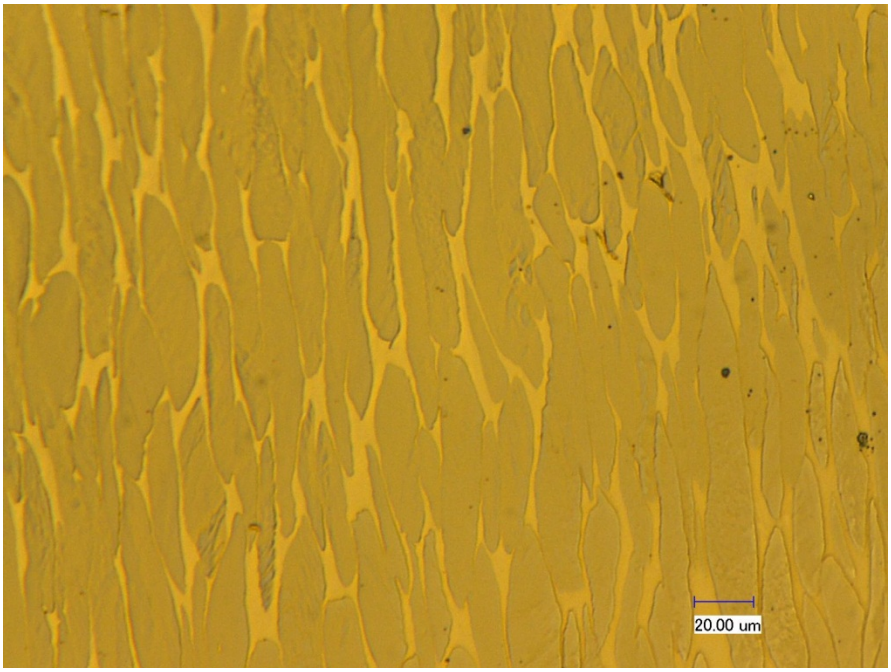

Figure 53 Microstructure of 1A processed WHA heat treated at 500C

Figure 54 and Figure 55 show microstructures of 1A processed samples heat treated at 700C and 900C. The hardness of these samples was 47.7 HRC and 44.1 HRC respectively. They have hardness values slightly less than 500 C samples. Also their microstructure shows some roughness at the boundaries, whereas the microstructures till 500C annealing are smooth.

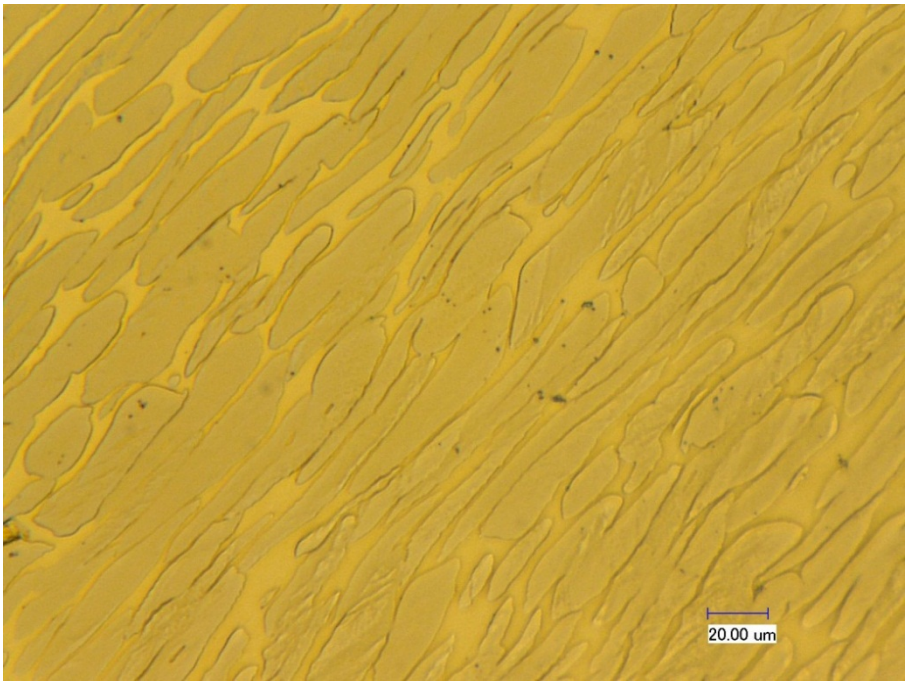

Figure 54 Microstructure of 1A processed WHA heat treated at 700C

Figure 55, Figure 56, Figure 57 and Figure 58 show microstructures of samples heat treated at 900C, 1100C, 1200C and 1300C. The microstructures show increased roughness at the boundaries as the heat treatment temperature goes up.

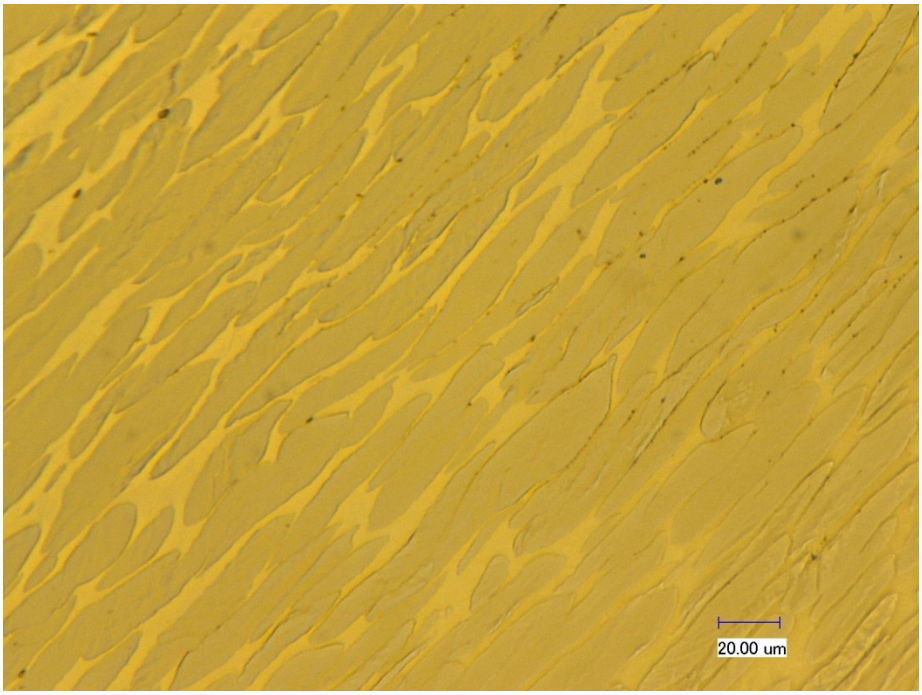

Figure 55 Microstructure of 1A processed WHA heat treated at 900c

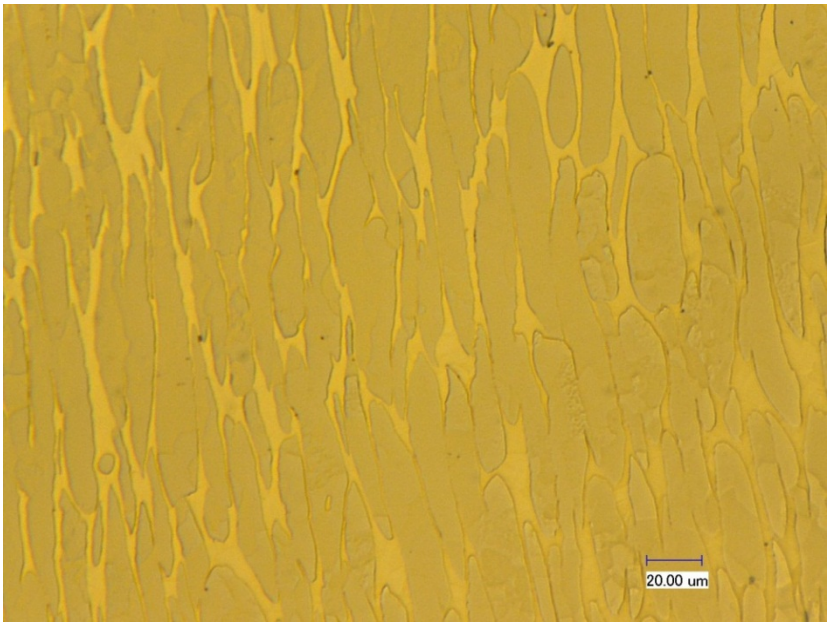

Figure 56 Microstructure of 1A processed WHA heat treated at 1100C

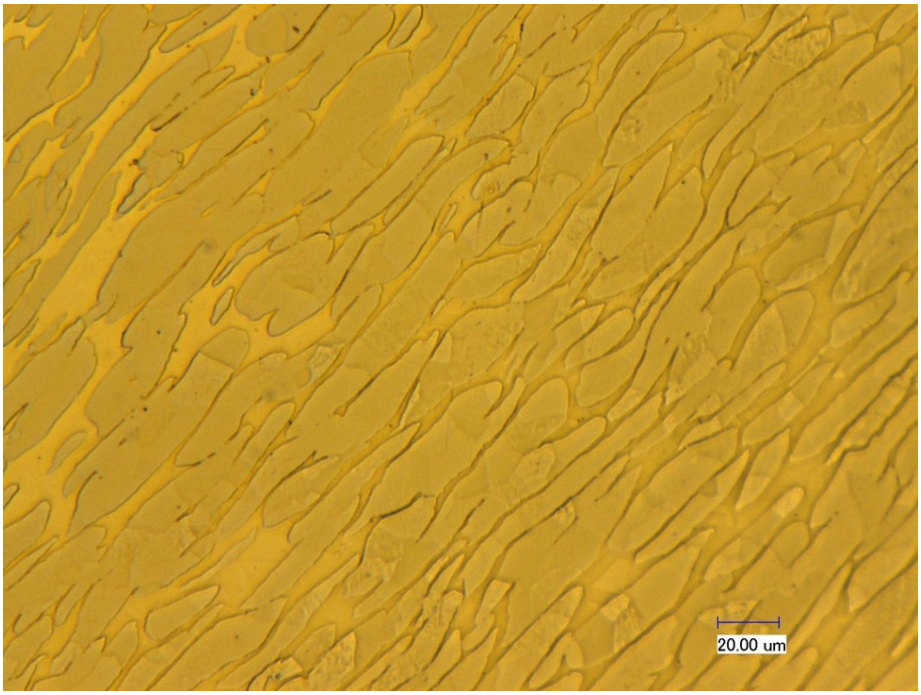

Figure 57 Microstructure of 1A processed WHA heat treated at 1200C

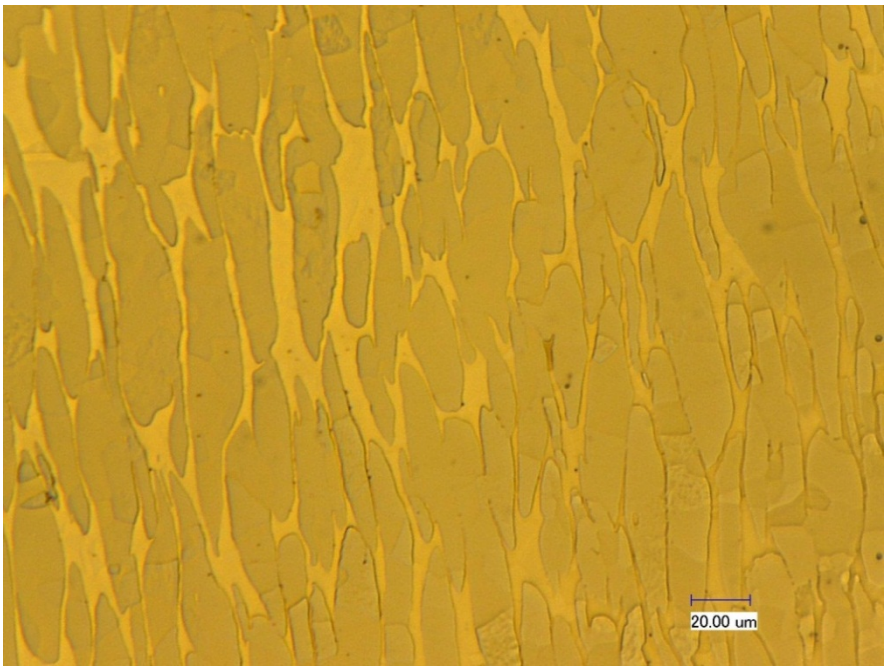

Figure 58 Microstructure of 1A processed WHA heat treated at 1300C

The difference in the roughness at the phase boundariesof1A processed sample and, 1Aprocessed material annealed at 1300C is shown in Figure 59.

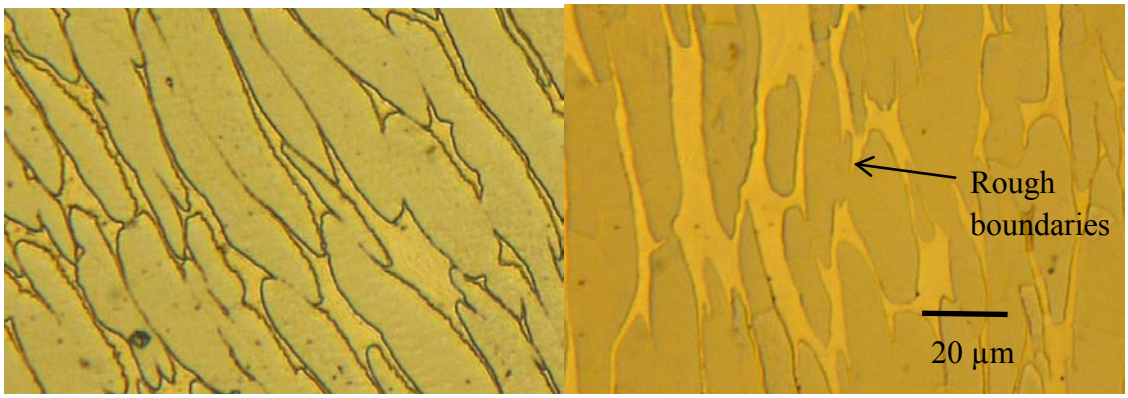

Figure 59 Microstructures of a) 1A processed sample and b) 1Aprocessed material annealed at 1300C, showing differences in roughness at phase boundaries

DISCUSSION

The material used in this project came from Aeroject Ordnance, Tennessee. The material was fabricated by liquid phase sintering at 1400C, in an inert hydrogen atmosphere. Tungsten heavy alloy systems are susceptible to oxidation of temperatures above 1000^0C. Thus for ECAE processing, the WHA billets were embedded in a stainless steel 316 billet of 0.25" thickness. The microstructure of the as received material reveals tungsten particles in the alloy are approximately spherical. The tungsten grain diameter ranged from 7μm – 45.5 μm. The distribution of tungsten particle sizes in the iron and nickel phase was non-uniform, which is typical of liquid phase sintering. Apart from this no other anomalies were observed. The effects of ECAE processing on microstructure and other properties are discussed in below.

ECAE

Though conceptually equal channel angular extrusion is a simple process, problems can arise during the processing. The use of sidewalls and a bottom slider allow for greater uniformity of work piece strain and enable a greater choice of materials. But at the same time, use of the moving components can introduce complexity into the processing if not handled properly.

The processing the tungsten heavy alloy billets encased in SS 316 containers of 0.25" wall thickness was challenging. The loads required for extrusion of these billets

approached the load capacity of the die used. This posed some problems while using the materials. High temperature and low temperature extrusions are discussed below.

High Temperature Extrusions

High temperature extrusions are extrusions done above 800C. Due to the nature of the hot-working steel used for the die in this project, the die could not be heated above 300C for long periods. As mentioned in the experimental procedures section the high temperatures extrusions were done at an extrusion rate of 0.5”/sec or 1”/sec to maintain isothermal conditions. The billets sheared during the extrusion, even at 1200^0C. Though the loads required for these extrusions were low, the high strain rates required to maintain the isothermal conditions caused the billets to shear. This observation is corroborated by Coates [49] who established a relation between shear localization and strain rate. This report was for 90W-7Ni-3Fewhereas the material examined in this project, was 90W-8Ni-2Fe. But the report published by Bose et al. [50] claims that the material is not strain rate sensitive above 600C, which was not the case in our extrusions. Due to the extrusion rate limit posed by isothermal conditions, no other extrusion rates were examined for our high temperature extrusions. All the extrusions at higher temperatures failed (i.e. shear localized) and low temperature extrusions were thus investigated.

Low Temperature Extrusions

The reports published by Islam et al. [51], Bose et al. [50] and Coates et al. [49] reported that the ductility of WHA alloy is a maximum at 300C and thus we attempted extrusions

at 300C. Because the die could be heated to 300C for prolonged periods of time, slower strain rates were possible. The stain rates used were 0.003”/sec and 0.001”/sec. Higher extrusion rates i.e. 0.005”/sec and above required higher loads, above 250 Kips which was above the load limit of the die. Successful single pass extrusions were consistent at 300C with extrusion rates of 0.003”/sec and 0.001”/sec.

Multiple passes at lower temperatures were challenging. We were unable to process single pass billets without intermediate annealing. This problem was also experienced by Valiev et al. [53]. Thus to avoid billet fracture during multi pass ECAE, the billets, which were enclosed in 316 steel, were annealed at 1300C for one hour.

Microstructure and Hardness Variation with ECAE

The as-received microstructure had spherical tungsten particles with an average diameter of 22μm with standard deviation of 8.5 μm. After the first pass, the tungsten grains change from spherical to oval. The average major and the minor axis lengths of this microstructure are 50.5 μm and 10.1 μm. The microstructure seemed to be more homogenous compared to the as-received microstructure. The hardness also increased from 25 HRC to 47.4 HRC. This was an expected result. After undergoing ECAE, the hardness increases were typical for “cold” ECAE processing. A second pass at 300C was not possible. To process the material through a second pass the material was annealed at 1300C.

The elongated grains which were obtained after the first pass resulted in a hardness of 47.4 HRC, which is higher than any other reported hardness for this alloy. Also, in the

reports published by Wei et al.[23] the orientation and aspect ratio of microstructure influences adiabatic shear banding. This paper reports that the elongated grains are conducive to adiabatic shear, which is required for kinetic energy penetrators. This might also be the reason for the challenges faced by us and also by Valiev et al. [53] multi-pass ECAE.

The second pass was a 2C pass; the microstructure obtained was as shown in Figure 42. This microstructure was termed “popcorn microstructure”. This is a novel microstructure and has not been reported in the literature to our knowledge. The hardness obtained with the “popcorn microstructure” is around 45.1 HRC which is nearly the same as the harness obtained after the first pass. The only microstructure which comes close this microstructure was reported by Baek et al. [48], who reported an increase in fracture toughness by about three times in an undulated microstructure (Figure 18) from the as-received spherical microstructure.

The third pass extrusion was 3E route. This was also done after an intermediate anneal at 1300C after the 2C pass. The hardness of this material was 47.3 HRC. This microstructure resembles the elongated microstructure of the first pass but the boundaries are not smooth but ragged. This microstructure is predicted to have nearly the same properties as the elongated as the elongated first pass material.

Microstructure Evolution

The microstructure from the as-received samples is spherical. Also the interface between the tungsten particles and the nickel-iron alloy matrix phase is smooth. After the first

pass, at 300 C and 0.003”/s the microstructure on the flow plane was examined. The tungsten particles were elongated as shown in Figure 36. This elongation is as expected. A square element after one pass ECAE is expected to elongate as shown in the literature review.

According to the literature review, a square element after 2C processing must regain its square shape. But in our project the circular tungsten particle was elongated to an oval shape on the flow plane. After 2C processing, the tungsten particles instead of regaining the circular shape, have the strange shape i.e. “popcorn microstructure”. The deviation from the theory is because these predictions are made for a homogenous material. The alloy system used in this project is not homogenous, but is a two phase metal-metal composite, and the tungsten particles are likely textured. The mechanical properties of the tungsten particle and the alloy matrix are different i.e. they have different plastic and elastic deformation behaviors. This inhomogeneity and texture of the tungsten particles coupled with the heat treatment done prior to the first pass extrusion leads to the “popcorn microstructure” of this material.

The microstructure of 3E processed tungsten heavy alloy is similar to that of one pass material. It possesses elongated grains with a rough interface between the tungsten particles and the matrix alloy phase. The elongation of grains follows the predicted theory for the 3E route, but the roughness arises from the previous microstructure and also the annealing of the samples before multi-pass processing.

Further extrusions were not done for these reasons: 1) the hardness was found to be constant after the first extrusion. 2) It was expected that further extrusions would give microstructures obtained before and 3) the project ended before more processing could be done.

Directionality of Mechanical Properties

The as-received microstructure has spherical tungsten particles. This kind of microstructure is presumed to have isotropic properties. After the first pass due to elongation of grains in one direction, anisotropicity is expected. The 2C processed material shows tungsten particle surface undulations, but by optical observation we can say that the tungsten particles appear randomly oriented. These samples, we believe will have near isotropic properties. Again after one more pass in the E direction (i.e. after 3E processing), the grains are elongated and this material is expected to have anisotropic properties.

Interfacial Behavior between Tungsten and Alloy Phase

The interface between the tungsten and the nickel iron alloy matrix also area affected by the ECAE processing. The interface between the tungsten and the alloy phase is inherently brittle [54] and this does not allow for shear localization in the tungsten phase[55].

Adiabatic Shear

The ability to undergo adiabatic shear is more likely to be seen in the elongated grains (1A and 3E processed) than the spherical (as-received) or the random “popcorn

microstructure" (2C processed). This is because shear bands are expected to form and propagate in the nickel-iron alloy matrix. The hindrance provided by the tungsten grains contains their growth. But in the elongated grains if the shear band formation is parallel to the major axis of the grains the material is more likely to undergo adiabatic shear. This was reported by Wei et al. This adiabatic shear banding enhances the self-sharpening behavior which is important for kinetic energy applications.

Recrystallization and Annealing

The recrystallization curve of single pass WHA was determined in this project. The recrystallization behavior is similar to that reported by Ekbom [33] and Islam [51]. Though these reports were on 90W-7Ni-3Fe and 95W-3.5Ni-1.5Fe the trend is the same.

The hardness of the tungsten heavy alloy did not change up to 300C. A slight increase was noticed at 500C. This can be attributed to the increase in hardness of tungsten particles. This increase in hardness was also found in the report published by Islam for 95W-3.5Ni-1.5Fe [51].

The hardness of the tungsten heavy alloy decreases slightly from 500C to 900C. This decrease is associated with softening of the Ni-Fe matrix phase. This observation is corroborated by the reports published by Ekbom [33], who reported that there is no loss of hardness of tungsten particles until about 900C. This result is also corroborated by the work done by Mathaudhu et al. [56] on recrystallization of tungsten.

From 900C to 1100C the hardness of the alloy decreases substantially from 44HRC to 31 HRC and levels off for annealing at higher temperatures. This decrease is due to the

decrease in the hardness of the tungsten particles. This behavior is also corroborated by the other reports [33, 51].

The microstructure of single pass material was examined for annealing from 300 – 1200 C. Figure 59 shows that difference in microstructure of the 1A processed sample vs. the sample at 1300C. The interface between tungsten particles and the alloy matrix is smooth in the single pass tungsten heavy alloy sample. But as the heat treatment temperature increases an observed roughness evolves between the tungsten particles and the alloy phase. The roughness increases as the annealing temperature increases and is pronounced at 1300C. No quantitative measurements were made, but this observation was obvious from visual inspection. This result is similar to the result obtained by Baek et al. [48], the undulation was generated in the grains by cyclic heat treatment. These undulated grains tend to have more impact energy due to the formation of local cracks, which dissipate energy. This microstructure is similar to the microstructure observed in 3E pass tungsten heavy alloy. The combination of elongation and undulation may be good for kinetic energy penetrators, but no such study was made and this might be of interest for future work.

XRD Results

The X-ray diffraction was done to check if any phase change occurred during the softening of the tungsten heavy alloy on annealing. XRD was done on as-received, 700 degree quenched and 1300C annealed samples. All the XRD images were nearly identical indicating no phase change occurred in the material during heat treatment.

CONCLUSIONS

From the results and observation made during this project the following conclusions can be made.

1. Single pass ECAE gives a morphology which is likely to be conducive to adiabatic shear banding.
2. The 2C processed tungsten heavy alloy has “popcorn” like morphology which is expected to have more toughness than conventional WHA morphology.
3. The 3E processed material may also be prone to adiabatic shear banding under high strain rate conditions and is expected to be tougher than 1A processed material.
4. A total strain of 3.4 was achieved in WHA, which is 1.5 times the maximum strain achieved previously in tungsten heavy alloys via ECAE. The deformation behavior of the material indicates higher strain levels are possible following a thermal mechanical processing sequence similar to that used in the study.
5. Intermediate annealing between ECAE passes combined with severe plastic strain are likely the causes for the “popcorn microstructure” seen in 2C material.

REFERENCES

[1] J.R.M. Spencer, James A., DTIC online information for the defense community, Gte Products Corp, Towanda Pa Chemical And Metallurgical Div, Washington D.C., (1991), pp. 1 - 233.

[2] B. Rabin, R. German, Metallurgical and Materials Transactions A, 19 (1988) 1523-1532.

[3] R.J. Dowding, Army Lab Command Watertown Material Technology Lab, U.S. Army Materials Technology Laboratory, Watertown, MA, (1991), pp. 1 - 17.

[4] A. Upadhyaya, Materials Chemistry and Physics, 67 (2001) 101-110.

[5] A.J. Delai, Proceedings of High Density Penetrator Materials Conf., Watertown, MA, 1977, pp. 102-107.

[6] J.M.N.S.P. Katlin, Proceedings of the High Density Penetrator Materials Conf, Watertown, MA, 1977, pp 55-63.

[7] S.P. Nowal, Proceedings of High Density Pentrator Materials Conference, Watertown, MA, 1977,pp. 42-49.

[8] D. Edmonds, P. Jones, Interfacial embrittlement in liquid-phase sintered tungsten heavy alloys, Metallurgical and Materials Transactions A, 10 (1979) 289-295.

[9] S.G. Caldwell, Tungsten Products an Allengheny Technologies Company, Allengheny Technologies, Madison

[10] R.Z. Valiev, I.V. Alexandrov, Nanostructured materials from severe plastic deformation, Nanostructured Materials, 12 (1999) 35-40.

[11] R.Z. Valiev, A.V. Korznikov, R.R. Mulyukov, Structure and properties of ultrafine-grained materials produced by severe plastic deformation, Materials Science and Engineering: A, 168 (1993) 141-148.

[12] L.C. S. Rusz, L.A. Dobrzanski, S. Tylsar, J. Kedron, ECAP methods application on selected non-ferrous metals and alloys, Archives of Materials Science and Engineering, 43 (2010) 69 - 76.

[13] D. Orlov, A. Reshetov, A. Synkov, V. Varyukhin, D. Lotsko, O. Sirko, N. Zakharova, A. Sharovsky, V. Voropaiev, Y. Milman, S. Synkov, Twist Extrusion as a Tool for Grain Refinement in Al-Mg-Sc-Zr Alloys, Y. Zhu, V. Varyukhin (Eds.)

Nanostructured Materials by High-Pressure Severe Plastic Deformation, Springer Netherlands,(2006), pp. 77-82.

[14] Y. Saito, H. Utsunomiya, N. Tsuji, T. Sakai, Novel ultra-high straining process for bulk materials—development of the accumulative roll-bonding (ARB) process, Acta Materialia, 47 (1999) 579-583.

[15] A. Rosochowski, L. Olejnik, Novel ultra-high straining process for bulk materials—development of the accumulative roll-bonding (ARB) process, Proceedings of the Institution of Mechanical Engineers, Part L: Journal of Materials: Design and Applications, 221, 2007, 187-196.

[16] V.M. Segal, A.E. Drobyshevky, V.I. Kopylov, Russ. Metall., 1 (1981) 971-974.

[17] A.A. Gazder, F.D. Torre, C.F. Gu, C.H.J. Davies, E.V. Pereloma, Microstructure and texture evolution of bcc and fcc metals subjected to equal channel angular extrusion, Materials Science and Engineering: A, 415 (2006) 126-139.

[18] I.J. Beyerlein, R.A. Lebensohn, C.N. Tomé, Modeling texture and microstructural evolution in the equal channel angular extrusion process, Materials Science and Engineering A, 345 (2003) 122-138.

[19] I.J. Beyerlein, C.N. Tomé, Analytical modeling of material flow in equal channel angular extrusion (ECAE), Materials Science and Engineering A, 380 (2004) 171-190.

[20] A. Mondal, A. Upadhyaya, Effect of heating mode and sintering temperature on the consolidation of 90W-7Ni-3Fe alloys, D. Agrawal, Journal of Alloys and Compounds, 509 (2011) 301-310.

[21] R. German, Liquid Phase Sintering, Plenum Press, New York, 1985.

[22] J. Das, G. Appa Rao, S.K. Pabi, Microstructure and mechanical properties of tungsten heavy alloys, Materials Science and Engineering: A, 527 (2010) 7841-7847.

[23] A.C. Bose, R. A. Langford, Development and properties of new tungsten- based composites for penetrators, Inter. J. Powder Metall, 28 (1992) 383-394.

[24] R.M. German, High Performance Heavy Alloys by Alloying and Process Control, Pennsylvania State Univ University Park Dept Of Materials Science And Enginee Ring, 1991, pp. 12.

[25] H. Couque, J. Lankford, A. Bose, Tensile fracture and shear localization under high loading rate in tungsten alloys, J. Phys. III France, 2 (1992) 2225-2238.

[26] J. Lankford, A. Bose and H. Couque, R. Asfahani, E.Chen and A. Crowson (Ed.) High strain rate behavior of refractory metals and alloys, TMS, Warrendale, PA, (1992), pp. 267.

[27] L.B. Radu Muresan, Study of the deformation and failure behavior of tungsten heavy alloys, Metalurgia International, 16 (2011) 34-41.

[28] W.D. Cai, A review of tungsten-based alloys as kinetic energy penetrator materials Reviews in particulate matter, 3 (1995) 71-131.

[29] Lee S, Magness, Jr., High strain rate deformation behaviors of kinetic energy penetrator materials during ballistic impact, Mechanics of Materials, 17 (1994) 147-154.

[30] R.M. German, Sintering Theory and Practice Wiley, New York, 1996.

[31] P.W. Voorhees, The theory of Ostwald ripening, Journal of Statistical Physics, 38 (1985) 231-252.

[32] R. German, A. Bose, S. Mani, Sintering time and atmosphere influences on the microstructure and mechanical properties of tungsten heavy alloys, Metallurgical and Materials Transactions A, 23 (1992) 211-219.

[33] L. Ekbom, T. Antonsson, Tungsten heavy alloy: deformation texture and recrystallization of tungsten particles, International Journal of Refractory Metals and Hard Materials, 20 (2002) 375-379.

[34] L.S. Magness, R.J.Dowling, A. Bose (Ed.), Tungsten and Refractory Metals, Metal Powder Industries Federation, Princeton, NJ, 1995, pp. 11–20.

[35] W.E. Gurwel, E.S.Chen, A. Crowson (Ed.) Proceedings of Tungsten and Tungsten Alloys Recent Advances, TMS, Warrendale, PA, 1991, pp. 43-52.

[36] R.J.D. P. Woolsey, K.J. Tauer, F.S. Hodi, Proceedings of Tungsten and Tungsten Alloys, Metal Powder Industries Federation, Princeton, NJ, 1992, pp. 533-540.

[37] A. Gsponer, Depleted-Uranium Wepons: the Whys and Wherefores, Independent Scientific Research Institute, Geneva, Switzerland, 2003, 1-33.

[38] L.S. Magness, R.J.Dowling. A. Bose (Ed.), Proceedings of Tungsten Refractory Metals and Alloys, Metal Powder Industries Federation, Princeton, NJ, 1996, pp. 133–144.

[39] L.S. Magness, Proceedings of Tungsten Refractory Metals and Alloys, Metal Powder Industries Federation, Princeton, NJ, 1998, pp. 41-58.

[40] R. Gero, L. Borukhin, I. Pikus, Some structural effects of plastic deformation on tungsten heavy metal alloys, Materials Science and Engineering A, 302 (2001) 162-167.

[41] Q. Wei, T. Jiao, K.T. Ramesh, E. Ma, L.J. Kecskes, L. Magness, R. Dowding, V.U. Kazykhanov, R.Z. Valiev, Mechanical behavior and dynamic failure of high-strength ultrafine grained tungsten under uniaxial compression, Acta Materialia, 54 (2006) 77-87.

[42] Q. Wei, H.T. Zhang, B.E. Schuster, K.T. Ramesh, R.Z. Valiev, L.J. Kecskes, R.J. Dowding, L. Magness, K. Cho, Mechanical behavior and dynamic failure of high-strength ultrafine grained tungsten under uniaxial compression, Acta Materialia, 54 (2006) 4079-4089.

[43] Z. Pan, Y. Guo, S. Mathaudhu, L. Kecskes, K. Hartwig, Q. Wei, Dynamic behaviors of body-centered cubic metals with ultrafine grained and nanocrystalline microstructures, Journal of Materials Science, 43 (2008) 7379-7384.

[44] Q. Wei, B.E. Schuster, S.N. Mathaudhu, K.T. Hartwig, L.J. Kecskes, R.J. Dowding, K.T. Ramesh, Quasi-static and dynamic mechanical properties of commercial-purity tungsten processed by ECAE at low temperatures, Materials Science and Engineering: A, 493 (2008) 58-64.

[45] R.Z.A. Valiev, I. V. Alexandrov, Nanostructures and enhanced propertiesin tungsten and its alloys processed by equal channel angular pressing, in, UFA state aviation technical univ (Russia), Inst of Physics of Advanced materials, (2001), pp. 22.

[46] V.M. Segal, Equal channel angular extrusion of flat products, Materials Science and Engineering: A, 476 (2008) 178-185.

[47] V.M. Segal, Materials processing by simple shear, Materials Science and Engineering A, 197 (1995) 157-164.

[48] M.-H.-H. Woon Hyung Baek, Eun-Pyo Kim, Heat Treatment Behavior of Tungsten Heavy Alloy, Solid State Phenomena, 118 (2006) 35-40

[49] R.S. Coates, K.T. Ramesh, The rate-dependent deformation of a tungsten heavy alloy, Materials Science and Engineering: A, 145 (1991) 159-166.

[50] A. Bose, D. Sims, R. German, Test temperature and strain rate effects on the properties of a tungsten heavy alloy, Metallurgical and Materials Transactions A, 19 (1988) 487-494.

[51] M.T. Syed Humail Islam, Xuan Hui Qu, Mechanical properties variation with test temperature for liquid phase sintered 95W-3.5Ni-1.5Fe alloys, Material Science Forum, 561-565 (2007) 647-650.

[52] J.Y. Zhigang Wei, Shisheng Hu, Yongchi Li, Infuence of microstructure on adiabatic shear localization of pre-twisted tungsten heavy alloys, International Journal of Impact Engineering, 24 (2000) 747-758.

[53] R.Z. Valiev, I. V. Alexandrov, Nanostructures and Enhanced Properties in Tungsten and its Alloys Processed by Equal Channel Angular Pressing, DTIC online information for the defense community, Ft. Belvoir, VA, 2002, pp. 22.

[54] D.-K. Kim, S. Lee, W. Hyung Baek, Microstructural study of adiabatic shear bands formed by high-speed impact in a tungsten heavy alloy penetratorMaterials Science and Engineering: A, 249 (1998) 197-205.

[55] D.-K. Kim, S. Lee, J.-W. Noh, Dynamic and quasi-static torsional behavior of tungsten heavy alloy specimens fabricated through sintering, heat-treatment, swaging and aging,Materials Science and Engineering: A, 247 (1998) 285-294.

[56] S.N. Mathaudhu, A.J. deRosset, K.T. Hartwig, L.J. Kecskes, Microstructures and recrystallization behavior of severely hot-deformed tungsten, Materials Science and Engineering: A, 503 (2009) 28-31.

VITA

Name:	Venkata Ravi Kiran Vasiraju
Address:	Department of Mechanical Engineering, College of Engineering, Texas A&M University 3123 TAMU College Station, TX 77843-4225
Email Address:	vvravikiran@gmail.com
Education:	B.E. Mechanical Engineering, Osmania University, 2008 Hyderabad, India